SWANSEA UNIVERSITY

College of Engineering

Research Dissertation. EG-M101.

Accurate high order FE solution of singular problems

by Ferran Gil.

Advisor: Dr. Rubén Sevilla

Swansea, December 2018

INDEX

1. Introduction 1

1.1. Objectives and overview 2

1.2. State of art 3

2. High-order Fem 5

2.1. FEM model problem 6

2.2. FEM weak formulation 6

2.3. Spatial discretization 7

Shape functions 8

Numerical integration 11

3. integrated singular basis function method (ISBFM). 12

3.1. ISBFM Model problem 14

3.2. ISBFM weak formulation 14

3.3. ISBFM spatial discretization 16

3.4. Numerical integration for singular functions 19

Quadratures for singular functions 19

Avoid the integrals with singular functions 19

3.5. Blending functions 21

4. Results 23

4.1. Mesh convergence 26

FEM convergence 26

ISBFM convergence 27

Motz problem convergence 29

4.2. Numerical integration 30

Non-singular functions 31

Singular functions 32

4.3. Singular functions added 34

4.4. Blending effect 35

Blending function 1 35

Blending function 2 38

4.5. Node and singularity placement 39

5. Conclusions 43

6. Future developments 45

7. References 46

1. INTRODUCTION

Since the origin of the FEM in the field of the structural analysis, as in other fields, singularities due to discontinuities in the boundary conditions or abrupt changes in the boundary shape have been a problem to solve. The crack-tip and inner corners are two well-known examples of singularities and non-smooth solutions in structural problems.

Usually, to achieve an acceptable accuracy in this kind of problems, the local refinement around the singularity is employed. However, the rate of convergence and the solution's accuracy is not reasonable [10].

Isoparametric FEM is the most popular method. Software as Ansys, Hypermesh, Abaqus, Apex, etc. are based in low-order *isoparametric FEM*. That is due to the easy and reduce cost to implementation the *isoparametric FEM* compared to other methods.

However, some fields like scattering or fluid dynamics need to use high-order methods and represent the geometry with high accuracy. This suppose a problem for the *isoparametric FEM*. The use of high-order *FEM* will increase computational cost, if the mesh size keeps. So, to not increase the computing time the elements size in the high-order mesh will be bigger than the elements size used in the low-order mesh [11]. Nonetheless, a coarse mesh leads to represent the geometry with not reasonable accuracy. Due to that, in the last decades many researches have been developing FEM methods that allows use high-order elements and represents with an acceptable accuracy the geometry of the problem without a high computational cost.

The used of high-order curved elements, called the p-version of *FEM* (*p-FEM*) [10], allows to obtain an exact boundary description without mesh refinement for high-order elements. However, *p-FEM* approximates the solution in reference element because define the polynomial interpolation in local coordinates (reference element) as the *isoparametric FEM* that implies a loss of consistency cause a local interpolation of degree $p > 1$ not correspond to polynomial interpolation in Cartesian coordinates [11].

Another FE methodologies have been assessed in order to solve this loss of consistency for $p > 1$. The *Cartesian* FEM doesn't use a reference element and defines the polynomial basis functions for the approximation of the solution directly in the physical space in Cartesian coordinates. Thus, each element needs a specific shape functions and quadratures for the numerical integration because there isn't a reference element and isoparametric transformation. That suppose an extra computational cost that is justified by the improved accuracy.

Then, *NURBS Enhanced Finite Element Method* (*NEFEM*) [9, 12] is developed in order to avoid geometric representation problems and loss of consistency due to isoparametric transformation. *NEFEM* represent the exact geometry of the problem by means of NURBS. Due to that, the elements' shape in contact with domain boundaries is defined with this kind of curves which use is extended in the industry. Moreover, in

NEFEM the polynomial basis functions are defined in Cartesian coordinates as occurs in *Cartesian FEM*. Thus, algorithms to build quadrature and shape functions for *NEFEM* elements have been developed in order to apply the *NEFEM*.

NEFEM allows to solve problems with high accuracy using coarse meshes and high-order elements, as it has been demonstrated in [9]. Nevertheless, NEFEM is not able to obtain a reasonable accuracy for problems in which the solution is non-smooth.

These problems that presents non-smooth solutions are not only in *NEFEM*. Due to that, some methods have been developed in order to avoid the refinement around the singularity to achieve a satisfactory accuracy.

In a field as numerical methods, improve the accuracy of solutions and reduce computing's times are main goals. There are many studies to pursue these aims and the main goal of this thesis is assess a method to solve singularity problems to determinate whether can be applied with *NEFEM* together.

1.1. Objectives and overview

This thesis focuses on assess a method which achieve reasonable accuracy for non-smooth solutions without mesh refinement. At this moment, *NEFEM* is not able to obtain reasonable accuracy for non-smooth solutions. Due to this fact, method that is capable to solve this kind of problems integrated in *NEFEM* would be an upgrade. And fields in which *NEFEM* would be an adequate option to apply would grow up.

The Integrated Singular Basis Function Method has been assessed. This method has been tested in order to known its accuracy to solve problems with non-smooth solutions in boundaries. A main goal of this thesis is evaluate the performance of the *ISBFM* in problems in which the use of *NEFEM* is considered adequate.

For this purpose, the following steps have been followed.

1. **Development of FEM code in Matlab.** As ISBFM is based on add the singular local solution to the ordinary basis functions, the first step has been developed a traditional *Isoparametric FEM* code. Verify the code before introduce the ISBFM was the first goal. In this step, singularities in the domain have not been introduced yet. Section 2 is devoted to the presentation of *FEM*. Weak formulation, shape functions and quadratures for this method have been detailed. The employ of Lagrange multipliers to impose the Dirichlet boundary conditions are introduced in this section. Besides, the difference among low order *FEM*, high order *FEM* and *NEFEM* have been shown.

2. **Implementation the *ISBFM* in the *FEM* code developed.** After verify that *FEM* code developed works properly, the *ISBFM* has been added to code. Weak formulation, shape functions and for *ISBFM* are shown in section 3. Moreover,

the numerical integration has been studied because singular functions appears in the formulation. The expansion of the linear system of equations introduced in section 2 due to the singular basis functions added is assessed in section 3. In this section the difference between traditional *FEM* and *ISBFM* can be observed. Otherwise, the effect of the employ of blending functions in order to smooth the influence of the singular basis functions in regions away from the singular point is studied.

3. **Test the code to understand the *ISBFM* performance.** In [1, 2] the *ISBFM* is developed to be employed using low order basis functions. Moreover, in both examples, crack-tip [1] and inner corner [2], the singularity coincides with a node. However, *NEFEM* used high order basis functions and the singular point location usually will not be coincident with a node. Due to that, the influence of the singular point location has been assessed as well the performance of the *ISBFM* with high order ordinary basis functions. Besides, crack-tip and inner corner are problems in which the boundaries conditions alongside the singularity's boundary are homogeneous. Nevertheless, the performance of *ISBFM* in problems in which this boundary conditions are not true is unknown. Due to that, the code developed has been tested in order to know the performance the *ISBFM* in anyone case, even in which boundary conditions are not homogeneous alongside singularity's boundary. In section Results4 the results of this tests are shown.

4. **Determine whether *ISBFM* integrated in *NEFEM* will be valid for obtain non-smooth solutions with reasonable accuracy.** There are different treatments to solve non-smooth solutions due to singularities in boundaries. Through the thesis, the performance of one of these methods (*ISBFM*) has been studied in order to determine whether *NEFEM* would be able to employ it to improve the accuracy obtained by *NEFEM* in this kind of singular problems in which the solution is non-smooth. Results obtained are shown in section 4. Finally, in section 5 is explained whether *ISBFM* is a valid method to integrate in *NEFEM*.

1.2. State of art

Problems that contain singularities which lead to non-smooth solution have been focussed by researchers in the last decades. These kind of problem suppose a challenge for the classical FE method considering that achieve an acceptable accuracy is not easy and it can need a high computational cost. Some methods to solve problems that present singularities are exposed next.

Among the methods that focus the problems with singularities on of them is the *hp-FEM* for singular perturbations [6, 7]. As it has been commented before, the accuracy of solution can be increased by two ways: refining the mesh and increasing the order of elements. This method applied both techniques near the singular points to improve the

accuracy of the approximated solution [8]. Thus, only the areas near to singular point on the boundaries are affected by this method, whereas the solution on the rest of the domain is computed by classical *FEM*.

Another example of this methods is the *Integrated Singular Basis Function Method* (*ISBFM*) [1, 2] which propose add the terms from the singular local solution to the ordinary basis functions in the FEM solution. The *ISBFM* developed by Lorraine G. Olson, Georgios C. Georgiou, and William W. Schultz in 1991 [1] is focused in problems in which the boundaries conditions alongside the singularity's boundary are homogeneous (crack-tip and inner corner). However, there are problems in which the solution around a singularity is non-smooth and the boundary conditions alongside the singularity's boundary are not homogeneous. And the performance of *ISBFM* for these problems is unknown.

On the other hand, the weak formulation showed in [1] is based in a simplified problem without body forces and traction forces. Besides, the method tested in [1, 2] used quadratic ordinary basis functions, meanwhile the performance of method using high-order elements is not showed.

Moreover, in the studies that have been done [1, 2] the singularity match with a node. Nonetheless, in some FE method like *NEFEM* the singularity could no match with node. So, the ISBFM performance when singularity doesn't match with a node is unknown too.

Other method employed to avoid singularities in the problem's solution is the *Generalized Finite Element Method* (*GFEM*) [4] which is based on the enrichment of the local basis functions in order to ensure a good local approximation. This method approximate the solution of a boundary value problem. Uses local spaces consisting of functions with the property that functions can accurately approximate the solution. Then a partition of unity is used to pasting these spaces together to form a good subspace approximation to ensure a good global solution approximated.

The *Extended Finite Element Method* [3, 5] is based on *GFEM* and the partition of unity method. This method extend the enrichment of the solution space with discontinuous functions. Thus, only nodes affected by the singularity are enriched. This method is usually used to solve problems such as crack propagation.

2. HIGH-ORDER FEM

The use of the technique of numerical analysis known as the Finite Element Method (FEM) has been popularized in the las decades thanks to the use of computers.

This technique allows solving common problems in engineering fields as mechanical problems, thermal, wave propagation, etc. These involve the integration of complex system of partial differential equations (PDE's), which until then were unapproachable, except in very simply cases. To solve these systems the MEF convert PDE system into another system of algebraic equations, whose resolutions by computers is relatively simply. However, this change induce errors that must been assumed.

Initially, a domain formed by an infinite number of points, is replaced by a domain formed by a finite number of points. This process is called spatial discretization and results in a mesh formed by elements and nodes.

On the domain, there are some governing equations that describes the behaviour of the physical phenomenon (mechanical equilibrium, heat transfer, etc.). As it happens in the analytical solutions, there is only one unique solution. Due to that some boundary conditions have to be imposed.

The unknown function (temperature, displacements, etc.) can be interpolated by means of the points obtained in the spatial discretization (usually matched with nodes) on which elementary basis functions are supported, called shape functions. These functions usually are polynomials. Moreover, *FEM* usually employs an isoparametric transformation which consists in transform each element of the mesh into a reference element build previously in order to use the same shape functions in whole domain. When these reference elements are used the method is called *isoparametric FEM*. The weak form of the governing equation allows to obtain the algebraic equation system mentioned before which will be solved after the boundary conditions have been imposed. That system is computed for each element of mesh and then it is assembled into the global system.

The weak form of the governing equations obtained induce errors. The shape functions used usually are polynomials functions which are not capable to represents the exact solution. Moreover, the spatial discretization don't represents the exact geometry of the problem. Due to these errors, mesh refinement (increase the number of elements that compose the domain) and increase the order of shape functions are methods used to improve the accuracy of solution. The second method, increase the order of shape functions, presents a higher convergence [10].

In this section it has been explained how to obtain the equation system to solve a PDE problem applying the *isoparametric FEM*.

2.1. FEM model problem

The partial differential equation considered to solve by FEM is a Poisson problem which is shown in (1). Problem is considered in a domain $\Omega \in R^2$ whose boundary is partitioned as $\partial\Omega = \Gamma_D \cup \Gamma_N$ with $\Gamma_D \cap \Gamma_N \neq 0$.

$$\begin{aligned} -\Delta u &= f \quad \text{in} \quad \Omega \\ u &= u_D \quad \text{on} \quad \Gamma_D \\ \overline{\nabla} u \cdot \overline{n} &= t \quad \text{on} \quad \Gamma_N \end{aligned} \tag{1}$$

The partial differential equation introduce in (1) corresponds to the strong form of the problem. To solve it by FEM is required to transform it to the weak form as is explained in [13]. Equation (1) has been employed as model problem to develop the following sections:

- In section 2.2 the steps to obtain the weak form are exposed. Meanwhile, in section 0 the spatial discretization, including shape functions and numerical integration, is presented.
- In section 3 is explained the ISBFM following the same steps followed in section 2 in order to note the difference between both methods.

2.2. FEM weak formulation

The first step to obtain the weak formulation is to transform the exact solution into an approximate solution as it is shown in equation (2):

$$u(x,y,z) = \sum_{j=1}^{n} u^j \cdot N^j(x,y,z) \tag{2}$$

Note that if the approximated functions form a complete set and $n = \infty$, the approximated solution will converge to the exact solution.

As it is explained in [13], multiplying the PDE by a test function ϕ and applying the divergence theorem leads to the weak formulation for the Poisson problem that is shown in equation (3):

$$\int_{\Omega} \overline{\nabla}\phi \cdot \overline{\nabla}u \cdot d\Omega = \int_{\Omega} \phi \cdot f \cdot d\Omega + \int_{\Gamma_N} \phi \cdot t \cdot d\Gamma_N \tag{3}$$

Dirichlet boundary conditions have been imposed into the approximated solution. In spite of that, they can be imposed by Lagrande multipliers as is explained in [14]. It will be useful to apply in section 3.2.

Then, equation (3) becomes into equations (4) and (5) after the essential boundary conditions are introduced employing Lagrange multipliers:

$$\int_{\Omega} \overline{\nabla}\phi \cdot \overline{\nabla}u \cdot d\Omega + \int_{\Gamma_D} \omega \cdot \lambda \cdot d\Gamma_D = \int_{\Omega} \phi \cdot f \cdot d\Omega + \int_{\Gamma_N} \phi \cdot t \cdot d\Gamma_N \tag{4}$$

$$\int_{\Gamma_D} \omega \cdot u \cdot d\Gamma_D = \int_{\Gamma_D} \omega \cdot u_D \cdot d\Gamma_D \tag{5}$$

2.3. Spatial discretization

After weak formulation has been obtained it's time to introduce the spatial discretization. Then, applying the Galerkin method [13], introducing the approximation of the solution in equation (2) and introducing the Lagrange multipliers as expanded in terms of basis functions, equations (4) and (5) leads to the following system of equations (6) and (7):

$$\begin{aligned} &\sum_{j=1}^{n} \left[\int_{\Omega} \overline{\nabla}N_i \cdot \overline{\nabla}N_j \cdot d\Omega \right] \cdot u_j + \sum_{j=1}^{n^\lambda} \left[\int_{\Gamma_D} N_i \cdot N_j^\lambda \cdot d\Gamma_D \right] \cdot \lambda_j \\ &= \int_{\Omega} N_i \cdot f \cdot d\Omega + \int_{\Gamma_N} N_i \cdot t \cdot d\Gamma_N \qquad \text{for } i = 1, 2, 3 \dots n \end{aligned} \tag{6}$$

$$\sum_{j=1}^{n} \left[\int_{\Gamma_D} N_i^\lambda \cdot N_j \cdot d\Gamma_D \right] \cdot u_j = \int_{\Gamma_D} N_i^\lambda \cdot u_D \cdot d\Gamma_D \qquad \text{for } i = 1, 2, 3 \dots n^\lambda \tag{7}$$

Note that n is the number of nodes in the domain and n^λ is the number of nodes on the Dirichlet boundaries.

The elementary functions used to introduce the Lagrange multipliers can be the same basis functions used in equation (2).

The system of equations (6) and (7) can be written in compact form as it is shown in (8):

$$\begin{bmatrix} \mathrm{K} & \mathrm{MK} \\ \mathrm{MK}' & 0 \end{bmatrix} \cdot \begin{Bmatrix} \overline{\mathrm{U}} \\ \Lambda \end{Bmatrix} = \begin{Bmatrix} \overline{\mathrm{F}} \\ \overline{\mathrm{F}_\lambda} \end{Bmatrix} \tag{8}$$

The matrices and vectors that are shown in (8) are the global matrices and vectors. They should be computed by assembling the elemental contributions which are shown in (9), (10), (11) and (12):

$$(\mathrm{K})_{\mathrm{ij}}^{\mathrm{e}} = \int_{\Omega_e} \overline{\nabla}\mathrm{N_i} \cdot \overline{\nabla}\mathrm{N_j} \cdot \mathrm{d}\Omega \quad \mathrm{K\ of\ dimension\ n \cdot n} \tag{9}$$

$$(\mathrm{MK})_{\mathrm{ij}}^{\mathrm{e}} = \int_{\partial\Omega_e \cap \Gamma_\mathrm{D}} \mathrm{N_i} \cdot \mathrm{N_j^\lambda} \cdot \mathrm{d}\Gamma_\mathrm{D} \quad \mathrm{MK\ of\ dimension\ n \cdot n^\lambda} \tag{10}$$

$$(\mathrm{F})_{\mathrm{i}}^{\mathrm{e}} = \int_{\Omega_e} \mathrm{N_i} \cdot \mathrm{f} \cdot \mathrm{d}\Omega + \int_{\partial\Omega_e \cap \Gamma_\mathrm{N}} \mathrm{N_i} \cdot \mathrm{t} \cdot \mathrm{d}\Gamma_\mathrm{N} \quad \mathrm{F\ of\ dimension\ n \cdot 1} \tag{11}$$

$$(\mathrm{F}_\lambda)_{\mathrm{i}}^{\mathrm{e}} = \int_{\partial\Omega_e \cap \Gamma_\mathrm{D}} \mathrm{N_i^\lambda} \cdot \mathrm{u_D} \cdot \mathrm{d}\Gamma_\mathrm{D} \quad \mathrm{F_\lambda\ of\ dimension\ n^\lambda \cdot 1} \tag{12}$$

Shape functions

Shape functions are used to approximate the solution as it's shown in equation (2). They have to be stablished for each element, but *isoparametric FEM* is based on the use of reference elements thus shape functions are only computed for the reference elements. Due to that, it is necessary to make a transformation for each element in the mesh to the reference element as it is shown in Figure 1. Therefore, the real element is defined, as equation (13) shows, by the coordinates of its nodes and the interpolation made. It is possible to employ different shape functions for the interpolation of coordinate nodes (13) and for the interpolation of approximated solution (2). However, the same nodes (isoparametric elements) and the same shape functions are usually used. Furthermore, it is necessary that the interpolation present continuity C^0 between elements, in order to achieve convergence.

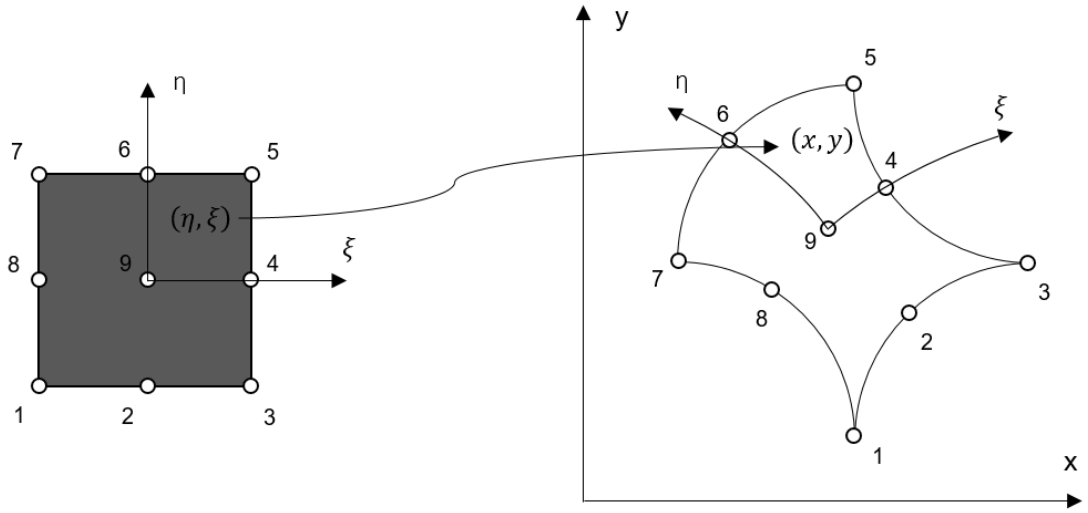

Figure 1. Reference element and real element [17]

$$x = \sum_{j=1}^{n} N^j(\xi, \eta, \tau) \cdot x^j$$

$$y = \sum_{j=1}^{n} N^j(\xi, \eta, \tau) \cdot y^j \quad (13)$$

$$z = \sum_{j=1}^{n} N^j(\xi, \eta, \tau) \cdot z^j$$

From equation (2) can be deduced that each shape function has value one in its associated node and zero in the rest as it is shown in equation *(14)*.

$$N^j(x^i, y^i, z^i) = \begin{cases} 1 & if \ \ i = j \\ 0 & if \ \ i \neq j \end{cases} \quad (14)$$

It is necessary that in each border of the element the interpolation depends exclusively on the shape functions of nodes belong to such border. Thus, the shape function associated with a node have to be null in the borders in which that node is not there.

Once the characteristics of the shape functions have been stablished, it is able to obtain the shape functions for an element. Then, considering a one-dimensional element defined by a number of nodes q, it can be defined the Lagrange polynomial associated with the node I as it is shown in equation (15).

$$L_I^{q-1}(\eta) = \frac{(x - x_1) \dots (x - x_{I-1})(x - x_{I+1}) \dots (x - x_q)}{(x_I - x_1) \dots (x_I - x_{I-1})(x_I - x_{I+1}) \dots (x_I - x_q)} \quad (15)$$

These polynomials (15) meet the necessary conditions defined for the shape functions. Then, shape functions for one-dimensional elements are Lagrange polynomials as it is shown in equation (16).

$$N_I(\eta) = L_I^{q-1}(\eta) \quad (16)$$

For quadrilateral and hexahedron elements their shape functions are made in base on Lagrange multipliers. This kind of elements, called Lagrange elements [17], has arranged the nodes (in contours and interior) in a regular mesh. Shape functions for quadrilateral and hexahedrons elements are defined as it is shown in equation (17) and equation (18) respectively.

$$N_{IJ}(\eta, \xi) = L_I^{q-1}(\eta) \cdot L_J^{q-1}(\xi) \quad (17)$$

$$N_{IJK}(\eta, \xi, \tau) = L_I^{q-1}(\eta) \cdot L_J^{q-1}(\xi) \cdot L_K^{q-1}(\tau) \quad (18)$$

Other shape functions can be made without use Lagrange polynomials. However, the shape functions of the Lagrange elements are easy to formulate and they have been used in this thesis in order to simplify the FEM code developed.

The one-dimensional reference element is defined in [-1 1] and has the nodes distributed uniformly. Reference element is defined in [-1 1] because it will be useful in order to compute the integrals by numerical integration as it will explained in section *Numerical integration*.

The integrals shown in equations (9), (10), (11) and (12) are computed in each element of mesh. When the transformation to the reference element is done it is necessary change the integral's domain as it is shown in equation (19).

$$\int_b^a f(x, y, z) \cdot \mathrm{d}\Omega = \int_{-1}^{1} f(\xi, \eta, \tau) \cdot |\mathrm{J}| \cdot \mathrm{d}\xi \mathrm{d}\eta \mathrm{d}\tau \quad (19)$$

Remark that Jacobian determinant is used to accommodate for the change coordinates as a multiplicative factor within the integral. The Jacobian matrix (20) is formed by all first-order partial derivatives of functions showed in equation (13).

$$J = \begin{bmatrix} \frac{\partial x}{\partial \xi} & \frac{\partial y}{\partial \xi} & \frac{\partial z}{\partial \xi} \\ \frac{\partial x}{\partial \eta} & \frac{\partial y}{\partial \eta} & \frac{\partial z}{\partial \eta} \\ \frac{\partial x}{\partial \tau} & \frac{\partial y}{\partial \tau} & \frac{\partial z}{\partial \tau} \end{bmatrix} \tag{20}$$

Numerical integration

The elemental matrices and vectors shown in (9), (10), (11) and (12) requires to compute of integrals in the domain and in the boundaries. The *FEM* programs have to solve them automatically, then numerical integration is the employed option.

Equation (21) shows that the integral of a function can be approximated as the sum of the evaluation of the function in a set of point multiplied by the associated weights.

$$\int_a^b f(x) \cdot dx \approx \sum_{i=1}^{n} f(x_i) \cdot w_i \tag{21}$$

A set of points and their associated weights is called a quadrature. In the *isoparametric FEM* is usually used the Gauss-Legendre quadrature which provide the minimum number of points to obtain the exact integration of polynomials up to a certain degree. Gauss-Legendre quadratures allows to exactly integrate all polynomials of degree $p \leq 2 \cdot n - 1$ where n is the number of points. How to obtain the quadratures for different degrees is explained in [15, 16].

Gauss-Legendre quadratures are frequently used. Due to that, these quadratures can be find in books or tables and they are usually given for the interval [1 -1] as the shape functions exposed in section *Shape functions*.

3. INTEGRATED SINGULAR BASIS FUNCTION METHOD (ISBFM).

The method proposed by Lorraine G. Olson, Georgios C. Georgiou, and William W. Schultz [1] has been assessed in order to solve problems that contain non-smooth singularities. The method proposed in [1] is adequate to solve problems in which the boundary conditions alongside the singularity's boundary are homogeneous. Besides, the formulation developed in [1] is based on a specific problem which no contains body forces, any traction forces and Neumann conditions are null in whole domain. Furthermore, the singularity's location match with a node and elements use are not high-order elements.

On the other hand, *NEFEM* tries to solve any kind of problem and then the conclusion obtained from [1] are not enough. Therefore, in this thesis it has been taken the main ideas proposed in [1] and they have been applied to Poisson problem defined in equation (1).

The main ideas that have been taken from [1] in order to do this thesis are:

- Divide the problem's solution that is calculated by FE method is two parts, one is the ordinary solution obtained by FEM and the other part satisfy the asymptotic solution and Laplace equation. Thus, equation (22) replaces equation (2). Due to that the method is called *Integrated Singular Basis Function Method*.

$$\mathrm{u} = \mathrm{u_r} + \mathrm{u_s} \approx \sum_{\mathrm{j=1}}^{\mathrm{n_r}} \mathrm{u_r^j} \cdot \mathrm{N_r^j} + \sum_{\mathrm{j=1}}^{\mathrm{n_s}} \mathrm{u_s^j} \cdot \mathrm{N_s^j} \tag{22}$$

  Note that the terms in equation (22) are:

  - u_r^j are the terms of regular solution.
  - N_r^j are the shape functions explained in section 0
  - n_r is the number of nodes.
  - u_s^j are the terms of asymptotic solution.
  - N_s^j are the shape functions used to expand the asymptotic solution.
  - n_s is the number of singular shape functions added.

- The shape functions used to expand the asymptotic solutions are defines by equation (23).

$$N_s^j = r^{(2j-1)/2} \cdot \cos\left[\left(\frac{2j-1}{2}\right) \cdot \theta\right] \quad \text{for } j = 1, 2, 3 \ldots n_s \tag{23}$$

Terms r and θ are the polar coordinates centred at the singular point.

Figure 2 shows the equation (23) for $j = 1$.

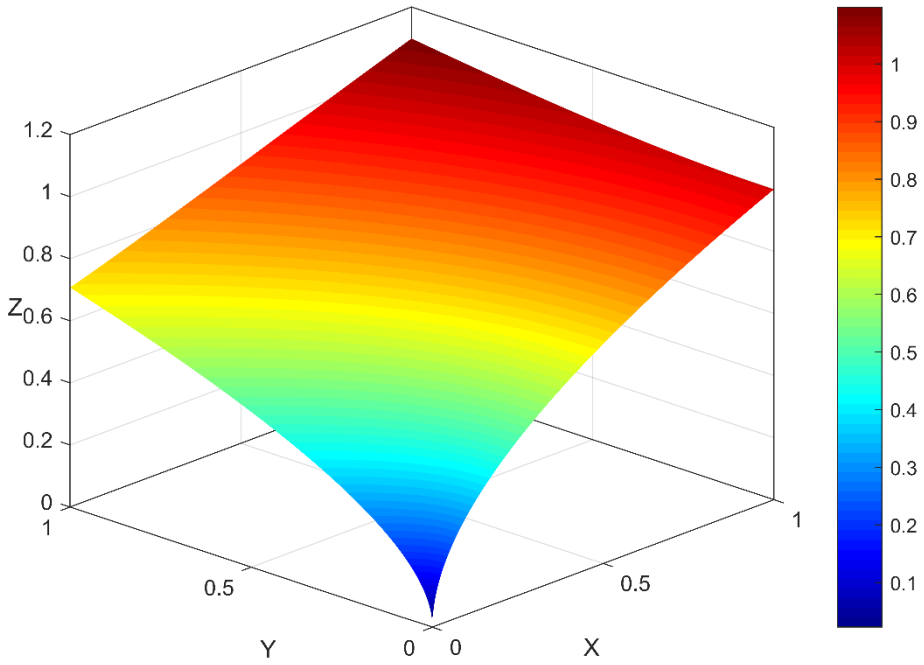

Figure 2. Singular function

Note that equation (23) satisfies:

- Laplace equation. $\Delta N_s^j = 0$.
- The boundary conditions due to the asymptotic solution along the boundary segments adjacent to the singular points are homogeneous.

Therefore, once the new equation to obtain the approximated solution by FEM has been established (22), the next step is update the strong form of the Poisson's problem defined in equation (1) (section 3.1). After that, the weak formulation and the spatial discretization will be developed again according to the new strong form in section 3.2 and in section 0 respectively. Moreover, section 3.4 is focussed in the numerical integration due to the singular functions that have appeared. Finally, in section 3.5

blending functions are assessed in order to reduce the influence of singular functions in far areas from the singularity.

3.1. ISBFM Model problem

The equation (1) becomes to equation (24) after separate the problem's solution in two parts as it is indicate in equation (22).

$$\begin{aligned} -\Delta u_r &= f \quad \text{in} \quad \Omega \\ u &= u_D - u_s \quad \text{on} \quad \Gamma_D \\ \overline{\nabla} u \cdot \overline{n} &= t - \overline{\nabla} u_s \cdot \overline{n} \quad \text{on} \quad \Gamma_N \end{aligned} \tag{24}$$

Furthermore, it is known that u_s satisfies the boundary conditions along the segments adjacent to the singular point. And writing $\Gamma_D = \Gamma_D^r + \Gamma_D^s$ and $\Gamma_N = \Gamma_N^r + \Gamma_N^s$ the strong form of the Poisson's problem becomes into equation (25).

$$\begin{aligned} -\Delta u_r &= f \quad \text{in} \quad \Omega \\ u_r &= u_D \quad \text{on} \quad \Gamma_D^s \\ u_r &= u_D - u_s \quad \text{on} \quad \Gamma_D^r \\ \overline{\nabla} u_r \cdot \overline{n} &= t \quad \text{on} \quad \Gamma_N^s \\ \overline{\nabla} u_r \cdot \overline{n} &= t - \overline{\nabla} u_s \cdot \overline{n} \quad \text{on} \quad \Gamma_N^r \end{aligned} \tag{25}$$

3.2. ISBFM weak formulation

As it has done in section 2.2, multiplying the PDE by attest function ϕ and applying the divergence theorem leads to the weak formulation for the Poisson's problem that it is shown in equation (26).

$$\int_\Omega \overline{\nabla}\phi \cdot \overline{\nabla} u_r \cdot d\Omega - \int_{\Gamma_N} \phi \cdot \overline{\nabla} u_r \cdot \overline{n} \cdot d\Gamma_N = \int_\Omega \phi \cdot f \cdot d\Omega \tag{26}$$

On the other hand, the Neumann's integral can be written in other terms, then equation (26) becomes into equation (27).

$$\int_{\Omega} \overline{\nabla}\phi \cdot \overline{\nabla} u_r \cdot d\Omega + \int_{\Gamma_N^r} \phi \cdot \overline{\nabla} u_s \cdot \overline{n} \cdot d\Gamma_N = \int_{\Omega} \phi \cdot f \cdot d\Omega + \int_{\Gamma_N} \phi \cdot t \cdot d\Gamma_N \tag{27}$$

Alternatively, the divergence theorem can be applied to the first domain integral as it is shown in equation (28). It avoids the need to compute singular functions in the domain Ω in case the test functions are replaced by the singular shape functions (23). In section 3.4 it has focussed on the integration of singular functions.

$$\begin{aligned} \int_{\Omega} \overline{\nabla}\phi \cdot \overline{\nabla} u_r \cdot d\Omega = &- \int_{\Omega} \Delta\phi \cdot u_r \cdot d\Omega + \int_{\Gamma_N} \left(\overline{\nabla}\phi \cdot \overline{n}\right) \cdot u_r \cdot d\Gamma_N \\ &+ \int_{\Gamma_D} \left(\overline{\nabla}\phi \cdot \overline{n}\right) \cdot u_r \cdot d\Gamma_D \end{aligned} \tag{28}$$

Applying the divergence theorem, equation (29) has been obtained.

$$\begin{aligned} &- \int_{\Omega} \Delta\phi \cdot u_r \cdot d\Omega + \int_{\Gamma_N} \left(\overline{\nabla}\phi \cdot \overline{n}\right) \cdot u_r \cdot d\Gamma_N + \int_{\Gamma_N^r} \phi \cdot \left(\overline{\nabla} u_s \cdot \overline{n}\right) \cdot d\Gamma_N \\ &- \int_{\Gamma_D^r} \left(\overline{\nabla}\phi \cdot \overline{n}\right) \cdot u_s \cdot d\Gamma_D = \int_{\Omega} \phi \cdot f \cdot d\Omega + \int_{\Gamma_N} \phi \cdot t \cdot d\Gamma_N \\ &- \int_{\Gamma_D} \left(\overline{\nabla}\phi \cdot \overline{n}\right) \cdot u_D \cdot d\Gamma_D \end{aligned} \tag{29}$$

Note that in equation (29) is not possible to apply essential boundary conditions directly due to u_s values in whole domain are unknown. Thus, it is necessary to impose them by Lagrange multipliers as it has been explained in section 2.2. Due to that, equations (27) and (29) are expanded, each one, into two equations.

Then, equation (27) becomes into equations (30) and (31).

$$\int_{\Omega} \overline{\nabla}\phi \cdot \overline{\nabla} u_r \cdot d\Omega + \int_{\Gamma_N^r} \phi \cdot \left(\overline{\nabla} u_s \cdot \overline{n}\right) \cdot d\Gamma_N + \int_{\Gamma_D} \omega \cdot \lambda \cdot d\Gamma_D = \int_{\Omega} \phi \cdot f \cdot d\Omega + \int_{\Gamma_N} \phi \cdot t \cdot d\Gamma_N \tag{30}$$

$$\int_{\Gamma_D} \omega \cdot u_r \cdot d\Gamma_D + \int_{\Gamma_D} \omega \cdot u_s \cdot d\Gamma_D = \int_{\Gamma_D} \omega \cdot u_D \cdot d\Gamma_D \tag{31}$$

and equation (29) becomes into equations (32) and again (31).

$$-\int_{\Omega} \Delta\phi \cdot u_r \cdot d\Omega + \int_{\Gamma_N} \left(\overline{\nabla}\phi \cdot \overline{n}\right) \cdot u_r \cdot d\Gamma_N + \int_{\Gamma_N^r} \phi \cdot \left(\overline{\nabla} u_s \cdot \overline{n}\right) \cdot d\Gamma_N - \int_{\Gamma_D^r} \left(\overline{\nabla}\phi \cdot \overline{n}\right) \cdot u_s \cdot d\Gamma_D + \int_{\Gamma_D} \omega \cdot \lambda \cdot d\Gamma_D = \int_{\Omega} \phi \cdot f \cdot d\Omega + \int_{\Gamma_N} \phi \cdot t \cdot d\Gamma_N - \int_{\Gamma_D} \left(\overline{\nabla}\phi \cdot \overline{n}\right) \cdot u_D \cdot d\Gamma_D \tag{32}$$

Thus, there are two weak formulations that defines the Poisson's problem (25) and one extra equation (31) in order to impose elementary conditions using Lagrange multipliers.

3.3. ISBFM spatial discretization

To establish the equation system to solve it is necessary to apply the Galerkin method and introduce the approximation solution defined in equation (22). This approximation is defined by two parts, the FE solution and the asymptotic singular solution. At this time, Galerkin method is applied by parts too.

On the one hand, Galerkin method is applied for the FE solution and the approximations of u_r and u_s are introduced in equations (30) and (31). Thus, chasing the space of test functions to be the same as the space of shape functions defined in section *Shape functions.*

On the other hand, Galerkin method is applied for the asymptotic singular solution and the approximations of u_r and u_s are introduced in equations (32) and (31).Thus, chasing the space of test functions to be the same as the space of singular shape

functions defined in equation (23). Note that the integral of domain in equation (32) will be null due to $\Delta N_s^j = 0$.

The system of equation obtained is shown in equations (33), (34) and (35).

$$\sum_{j=1}^{n_r}\left[\int_\Omega \overline{\nabla} N_r^i \cdot \overline{\nabla} N_r^j \cdot d\Omega\right]\cdot u_r^j + \sum_{j=1}^{n_s}\left[\int_{\Gamma_N^r} N_r^i \cdot \left(\overline{\nabla} N_s^j \cdot \overline{n}\right)\cdot d\Gamma_N\right]\cdot u_s^j + \sum_{j=1}^{n^\lambda}\left[\int_{\Gamma_D} N_r^i \cdot N_\lambda^j \cdot d\Gamma_D\right]\cdot \lambda^j = \int_\Omega N_r^i \cdot f \cdot d\Omega + \int_{\Gamma_N} N_r^i \cdot t \cdot d\Gamma_N \quad (33)$$

$$\text{for } i = 1, 2, 3 \dots n_r$$

$$\sum_{j=1}^{n_r}\left[\int_{\Gamma_N^r}\left(\overline{\nabla} N_s^i \cdot \overline{n}\right)\cdot N_r^j \cdot d\Gamma_N\right]\cdot u_r^j + \sum_{j=1}^{n_s}\left[\int_{\Gamma_N^r} N_s^i \cdot \left(\overline{\nabla} N_s^j \cdot \overline{n}\right)\cdot d\Gamma_N - \int_{\Gamma_D^r}\left(\overline{\nabla} N_s^i \cdot \overline{n}\right)\cdot N_s^j \cdot d\Gamma_D\right]\cdot u_s^j + \sum_{j=1}^{n^\lambda}\left[\int_{\Gamma_D} N_s^i \cdot N_\lambda^j \cdot d\Gamma_D\right]\cdot \lambda^j \quad (34)$$

$$= \int_\Omega N_s^i \cdot f \cdot d\Omega + \int_{\Gamma_N} N_s^i \cdot t \cdot d\Gamma_N - \int_{\Gamma_D}\left(\overline{\nabla} N_s^i \cdot \overline{n}\right)\cdot u_D \cdot d\Gamma_D$$

$$\text{for } i = 1, 2, 3 \dots n_s$$

$$\sum_{j=1}^{n_r}\left[\int_{\Gamma_D} N_\lambda^i \cdot N_r^j \cdot d\Gamma_D\right]\cdot u_r^j + \sum_{j=1}^{n_s}\left[\int_{\Gamma_D} N_\lambda^i \cdot N_s^j \cdot d\Gamma_D\right]\cdot u_s^j = \int_{\Gamma_D} N_i^\lambda \cdot u_D \cdot d\Gamma_D \quad \text{for } i = 1, 2, 3 \dots n_\lambda \quad (35)$$

Note that the discrete equation (33) has been obtained from equation (30) whereas the discrete equation (34) has been obtained from equation (32). And finally, the discrete equation (35) has been obtained from equation (31).

As it has been done in section 2.2, the system of equations (33), (34) and (35) can be written in compact form as it is shown in (36).

$$\begin{bmatrix} \mathrm{K} & \mathrm{KC} & \mathrm{MK} \\ \mathrm{KC}' & \mathrm{C} & \mathrm{MC} \\ \mathrm{MK}' & \mathrm{MC}' & 0 \end{bmatrix} \cdot \begin{Bmatrix} \overline{\mathrm{U_r}} \\ \overline{\mathrm{U_s}} \\ \Lambda \end{Bmatrix} = \begin{Bmatrix} \overline{\mathrm{F_r}} \\ \overline{\mathrm{F_s}} \\ \overline{\mathrm{F_\lambda}} \end{Bmatrix} \tag{36}$$

The equation system shown in (36) include the matrix and vectors of equation system (8). The new terms that turn up are due to the asymptotic solution added to the approximation of solution defined in equation (22). Each matrix and vector should be computed by assembling the elemental contributions. Matrix K, matrix MK, vector $\overline{\mathrm{F_r}}$ and vector $\overline{\mathrm{F_\lambda}}$ have been defined previously in equations (9), (10), (11) and (12) respectively. Remark that u solution calculated in (8) correspond to the FE solution $\mathrm{u_r}$ in (36).

Whereas the other terms of (36) are defined in equations (37), (38), (39) and (40).

$$(\mathrm{KC})_{\mathrm{ij}}^{\mathrm{e}} = \int_{\partial\Omega_{\mathrm{e}} \cap \Gamma_{\mathrm{N}}^{\mathrm{r}}} \mathrm{N_r^i} \cdot \left(\overline{\nabla}\mathrm{N_s^j} \cdot \overline{\mathrm{n}}\right) \cdot \mathrm{d}\Gamma_{\mathrm{N}} \quad \mathrm{KC\ of\ dimension\ } \mathrm{n_r} \cdot \mathrm{n_s} \tag{37}$$

$$(\mathrm{C})_{\mathrm{ij}}^{\mathrm{e}} = \int_{\partial\Omega_{\mathrm{e}} \cap \Gamma_{\mathrm{N}}^{\mathrm{r}}} \mathrm{N_s^i} \cdot \left(\overline{\nabla}\mathrm{N_s^j} \cdot \overline{\mathrm{n}}\right) \cdot \mathrm{d}\Gamma_{\mathrm{N}} - \int_{\partial\Omega_{\mathrm{e}} \cap \Gamma_{\mathrm{D}}^{\mathrm{r}}} \left(\overline{\nabla}\mathrm{N_s^i} \cdot \overline{\mathrm{n}}\right) \cdot \mathrm{N_s^j} \cdot \mathrm{d}\Gamma_{\mathrm{D}} \tag{38}$$

$$\mathrm{C\ of\ dimension\ } \mathrm{n_s} \cdot \mathrm{n_s}$$

$$(\mathrm{MC})_{\mathrm{ij}}^{\mathrm{e}} = \int_{\partial\Omega_e \cap \Gamma_{\mathrm{D}}} \mathrm{N_s^i} \cdot \mathrm{N_j^\lambda} \cdot \mathrm{d}\Gamma_{\mathrm{D}} \quad \mathrm{MC\ of\ dimension\ } \mathrm{n_s} \cdot \mathrm{n_\lambda} \tag{39}$$

$$\begin{aligned} (\mathrm{F_s})_{\mathrm{i}}^{\mathrm{e}} &= \int_{\Omega_e} \mathrm{N_s^i} \cdot \mathrm{f} \cdot \mathrm{d}\Omega + \int_{\partial\Omega_e \cap \Gamma_{\mathrm{N}}} \mathrm{N_s^i} \cdot \mathrm{t} \cdot \mathrm{d}\Gamma_{\mathrm{N}} \\ &- \int_{\partial\Omega_e \cap \Gamma_{\mathrm{D}}} \left(\overline{\nabla}\mathrm{N_s^i} \cdot \overline{\mathrm{n}}\right) \cdot \mathrm{u_D} \cdot \mathrm{d}\Gamma_{\mathrm{D}} \ \ \mathrm{F_s\ of\ dimension\ } \mathrm{n_s} \cdot 1 \end{aligned} \tag{40}$$

Note that in equation (40) there is an integral with a singular function. This kind of integral has been studied in section 3.4.

3.4. Numerical integration for singular functions

The method proposed in [1] doesn't need other quadratures than Gauss-Legendre quadrature that has been exposed in section 0. That is due to it is not necessary to compute any integral with singular function because the boundary conditions in segments adjacent to singularity are homogeneous. Thus in equation (40) there isn't an integral with singular function because the domain change from $\partial\Omega_e \cap \Gamma_D$ to $\partial\Omega_e \cap \Gamma_D^r$. Moreover, equation (29) is obtained in order to avoid the integral with singular function in the whole domain Ω.

However whether the problem to solve is a general case like it has been defined in this thesis, it's necessary to compute an integral with singular functions. That suppose an increment of computational cost due to the need of use specific quadratures with high number of points to integrate singular functions. Thus, it have been proposed two options: use specific quadratures for singular functions or change the problem to obtain homogeneous boundary conditions in the segments adjacent to singularity.

Quadratures for singular functions

The need of compute integrals with singular functions appears in several problems. As a consequence of that, many researches have been worked in many ways to solve it. Most of them are focussed in build quadratures with a high number of points around the singularity, two examples are shown in [18] and [19].

However, quadratures for *NEFEM* elements are not easy to make as it is shown in [9, 12]. Thus, the algorithms proposed to make them should be updated in order to include a method which can solve integrals with singular functions.

In this thesis, the goal to achieve is know the performance of ISBFM in a general case. Then, special quadratures for singular functions have not implemented in the code developed in order to solve the integrals with singular functions, but the number of points of Gauss-Legendre quadratures used have been increased considerably. This is because to assess the ISBFM's performance are not necessary this kind of quadratures, whereas quadratures for singular functions and NEFEM deserve a specific research way.

Avoid the integrals with singular functions

The integral with a singular function appears in equation (40). That can be avoid if the integral's domain is changed from $\partial\Omega_e \cap \Gamma_D$ to $\partial\Omega_e \cap \Gamma_D^r$. Thus, it is necessary to change the problem definition (25) in order to make $u_r = 0$ on Γ_D^s. To achieve it, it has been defined an expanded $u_r{}^*$ as it is shown in equation (41).

$$u_r{}^* = u_r - \widehat{u_D} \tag{41}$$

Where $\widehat{u_D}$ is define in (42).

$$\widehat{u_D} = \Big|_{\Gamma_D^s} u_D \tag{42}$$

As a consequence of that, the problem defines in (25) becomes into (43). This change allows to have $u_r = 0$ on Γ_D^s, but the vector $\overline{F_r}$ and the vector $\overline{F_s}$ that have been defined previously in (11) and (40) have become into (44) and (45).

$$\begin{aligned} -\Delta u_r &= f - \Delta\widehat{u_D} \quad \text{in} \quad \Omega \\ u_r &= 0 \quad \text{on} \quad \Gamma_D^s \\ u_r &= (u_D - \widehat{u_D}) - u_s \quad \text{on} \quad \Gamma_D^r \\ \overline{\nabla} u_r \cdot \overline{n} &= \left(t - \overline{\nabla}\widehat{u_D} \cdot \overline{n}\right) \quad \text{on} \quad \Gamma_N^s \\ \overline{\nabla} u_r \cdot \overline{n} &= \left(t - \overline{\nabla}\widehat{u_D} \cdot \overline{n}\right) - \overline{\nabla} u_s \cdot \overline{n} \quad \text{on} \quad \Gamma_N^r \end{aligned} \tag{43}$$

$$(F_r)_i^e = \int_{\Omega_e} N_r^i \cdot (f - \Delta\widehat{u_D}) \cdot d\Omega \; + \int_{\partial\Omega_e \cap \Gamma_N} N_r^i \cdot \left(t - \overline{\nabla}\widehat{u_D} \cdot \overline{n}\right) \cdot d\Gamma_N \tag{44}$$

$$F \text{ of dimension } n_r \cdot 1$$

$$\begin{aligned} (F_s)_i^e = &\int_{\Omega_e} N_s^i \cdot (f - \Delta\widehat{u_D}) \cdot d\Omega + \int_{\partial\Omega_e \cap \Gamma_N} N_s^i \cdot \left(t - \overline{\nabla}\widehat{u_D} \cdot \overline{n}\right) \cdot d\Gamma_N \\ &- \int_{\partial\Omega_e \cap \Gamma_D^r} \left(\overline{\nabla} N_s^i \cdot \overline{n}\right) \cdot u_D \cdot d\Gamma_D \quad F_s \text{ of dimension } n_s \cdot 1 \end{aligned} \tag{45}$$

Remark that this change maybe is not possible to apply in all cases. Because of that the first option, introduce specific quadratures for singular functions, is a better option. On the other hand, the most common problems with singularities in mechanical engineering are the crack-tip and inner corner problems. Both problems, have homogeneous boundary conditions along the segments adjacent the singularity, thus u_r and $\overline{\nabla} u_r \cdot \overline{n}$ are null in Γ_D^s and Γ_N^s respectively.

3.5. Blending functions

Solve the equation system defined in (36) entail an extra computational cost. Due to that, in [1] it is proposed the use of blending functions in order to restrict the influence of singularity in the whole domain. The blending functions determines the area which is affected by singularity and reduce the singularity's effect with the distance to singularity.

However, it has been demonstrated in [1] that the use of blending functions leads to a loss of accuracy. Nevertheless, the effect of used blending functions and high-order elements has not been assessed. Thus, in this thesis the effect of blending functions has been studied for low and high-order elements. Two blending functions proposed in [1] have been used and they are shown in equations (46) and (47).

$$W_1 = \frac{1}{R^3} \cdot (r - R)^2 \cdot (2r + R) \tag{46}$$

$$W_2 = \left(1 - \frac{x^2}{R^2}\right) \cdot \left(1 - \frac{y^2}{R^2}\right) \tag{47}$$

Note that R determines the limit of the singularity effect. Thus, when a blending functions is applied the equation (23) that defines the singular shape functions becomes to equation (48).

$$N_s^j = W_i \cdot r^{(2j-1)/2} \cdot \cos\left[\left(\frac{2j-1}{2}\right) \cdot \theta\right] \quad \text{for } j = 1, 2, 3 \dots n_s \tag{48}$$

In Figure 3 is shown the equation (46) with $R = 32$. It can be appreciated that the start and the end of function shown in Figure 3 is smooth in order to reduce the effects of blending function in this areas. Note that the derivate of function defined in (46) for $r = 0$ and $r = R$ is null.

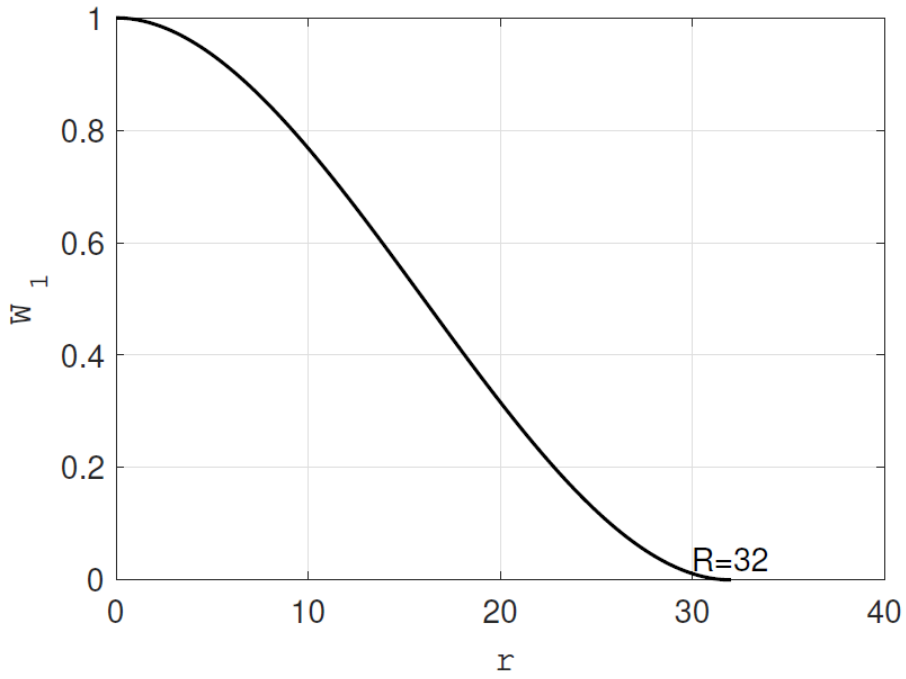

Figure 3. Blending function W_1 with R = 32.

4. RESULTS

Once the equation system to solve problems with non-smooth solutions by *FEM* has been established in (36) and Matlab code has been developed, it has been proceed to test the *ISBFM*. Three different problems have been used in order to test the *ISBFM* code developed in order to know its performance.

- First, the *isoparametric FEM* code have been tested. To do that, the method of manufactured solution have been employed. This method consists in impose an analytical solution known and obtain the strong form of the problem from this. So, the analytical solution is shown in (49) and the strong form of the problem is shown in (50).

$$\mathrm{u} = \cos(2 \cdot \mathrm{x} + \mathrm{y}) \text{ in } \quad \Omega \tag{49}$$

$$\begin{aligned} -\Delta \mathrm{u}_{\mathrm{r}} &= -5 \cdot \cos(2 \cdot \mathrm{x} + \mathrm{y}) \quad \text{in} \quad \Omega \\ \mathrm{u} &= \cos(2 \cdot \mathrm{x} + \mathrm{y}) \quad \text{on} \quad \Gamma_{\mathrm{D}} \\ \overline{\nabla}\mathrm{u} \cdot \overline{\mathrm{n}} &= [-2 \cdot sin(2 \cdot \mathrm{x} + \mathrm{y}), -sin(2 \cdot \mathrm{x} + \mathrm{y})] \cdot \overline{\mathrm{n}} \quad \text{on} \quad \Gamma_{\mathrm{N}} \end{aligned} \tag{50}$$

Figure 4 shows the analytical solution defined in (49).

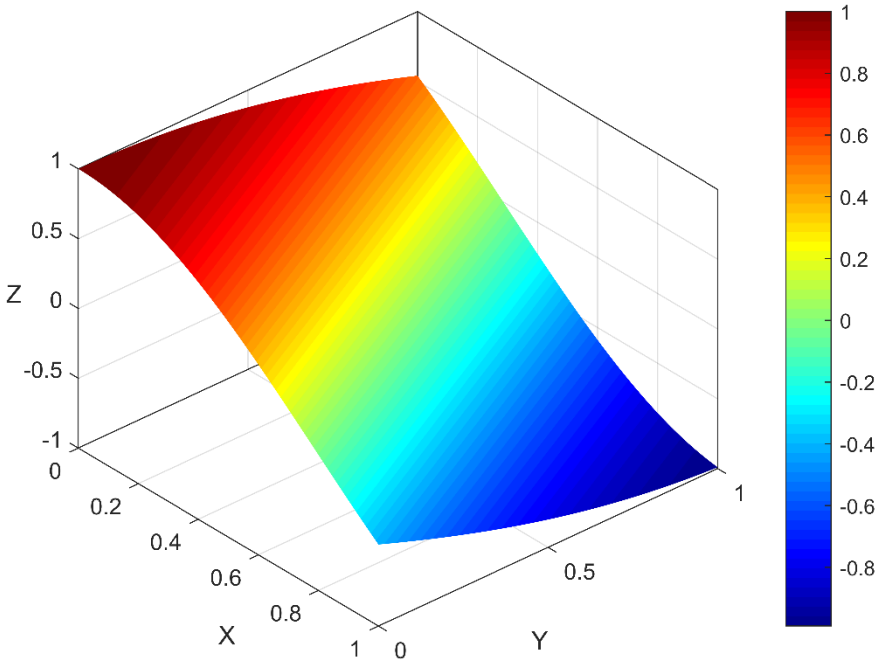

Figure 4. FEM problem

- The second step has been introduce a singularity in the solution manufactured, the singularity has been located in [0.5 0]. To do that, the equation defined in (23) has been added to the solution (51). The strong form of the problem is shown in (52).

$$\mathrm{u} = u_r + u_s = \cos(2 \cdot \mathrm{x} + \mathrm{y}) + \sum_{j=1}^{n_s} \mathrm{N_s^j} \text{ in } \quad \Omega \tag{51}$$

$$\begin{aligned} -\Delta \mathrm{u_r} &= -5 \cdot \cos(2 \cdot \mathrm{x} + \mathrm{y}) \quad \text{in} \quad \Omega \\ \mathrm{u_r} &= \cos(2 \cdot \mathrm{x} + \mathrm{y}) \quad \text{on} \quad \Gamma_\mathrm{D}^\mathrm{s} \\ \mathrm{u_r} &= \cos(2 \cdot \mathrm{x} + \mathrm{y}) - \mathrm{u_s} \quad \text{on} \quad \Gamma_\mathrm{D}^\mathrm{r} \\ \overline{\nabla} \mathrm{u_r} \cdot \overline{\mathrm{n}} &= [-2 \cdot sin(2 \cdot \mathrm{x} + \mathrm{y}), -sin(2 \cdot \mathrm{x} + \mathrm{y})] \cdot \overline{\mathrm{n}} \quad \text{on} \quad \Gamma_\mathrm{N}^\mathrm{s} \\ \overline{\nabla} \mathrm{u_r} \cdot \overline{\mathrm{n}} &= [-2 \cdot sin(2 \cdot \mathrm{x} + \mathrm{y}), -sin(2 \cdot \mathrm{x} + \mathrm{y})] \cdot \overline{\mathrm{n}} - \overline{\nabla} \mathrm{u_s} \cdot \overline{\mathrm{n}} \\ \text{on} \quad & \Gamma_\mathrm{N}^\mathrm{r} \end{aligned} \tag{52}$$

Figure 5 shows the analytical solution defined in (51) for $\mathrm{j} = 1$.

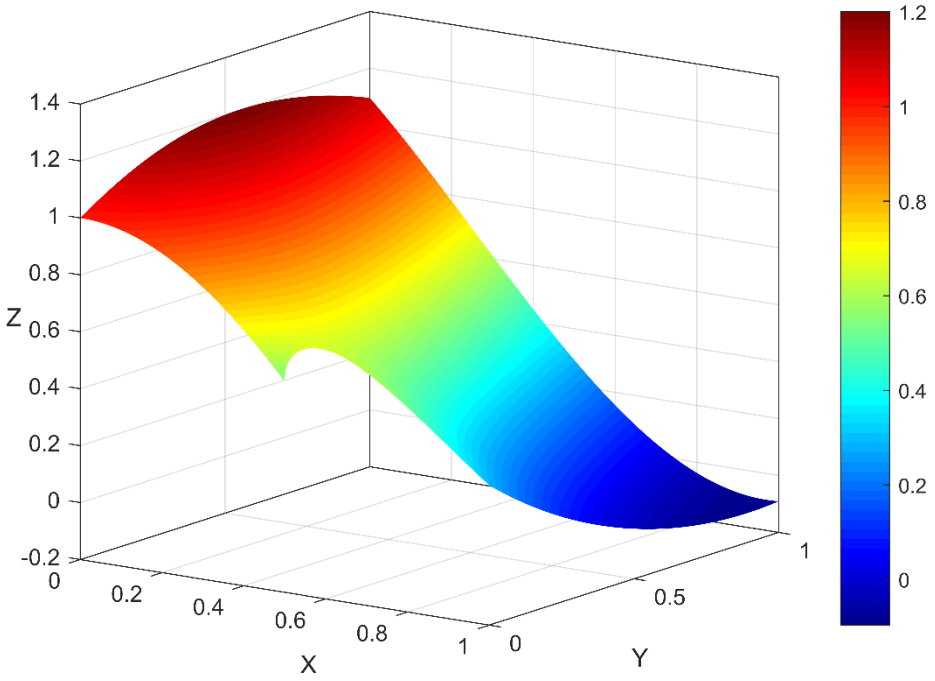

Figure 5. ISBFM problem

Note that this problem have to be solved using special numerical integration for singular functions as it has been explained in section *Quadratures for singular functions*. It isn't possible to modify the problem as it is proposed in section *Avoid the integrals with singular functions* because if it is done, the problem would become into (53) and solve these problem doesn't have a sense.

$$
\begin{aligned}
-\Delta u_r = \ & \text{in} \quad \Omega \\
u_r = 0 \ & \text{on} \quad \Gamma_D^s \\
u_r = -u_s \ & \text{on} \quad \Gamma_D^r \\
\overline{\nabla} u_r \cdot \overline{n} = 0 \ & \text{on} \quad \Gamma_N^s \\
\overline{\nabla} u_r \cdot \overline{n} = -\overline{\nabla} u_s \cdot \overline{n} \ & \text{on} \quad \Gamma_N^r
\end{aligned}
\tag{53}
$$

Due to the problem exposed in (53) doesn't have sense, and the goal of this thesis it's evaluate the ISBFM formulation, the problem exposed in (52) has solved by two ways:

- Using a high number of points in the numerical integration with Gauss-Legendre quadrature.
- Applying j > 2 in equation (23) to avoid the singular function. These problem allows to test the formulation implemented.

- Finally, the Motz problem proposed in [1] has been solved, in spite of this problem is a specific case. Figure 6. Motz problem shows the problem.

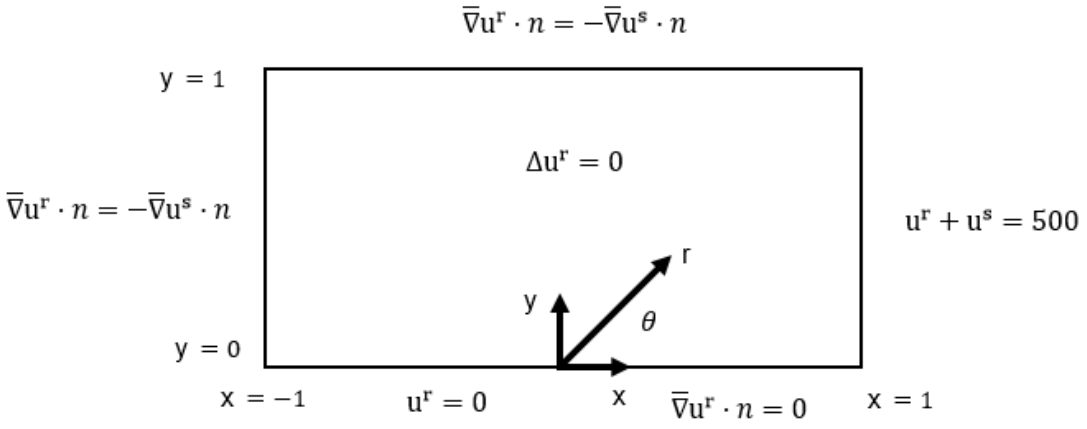

Figure 6. Motz problem

By other hand, the following tests have been done in order to evaluate the *ISBFM* formulation implemented in the code that has been developed.

- Mesh convergence for the following problems
    - Test the FE code. Problem (50) is solved
    - Test the ISBFM code. Problem (52) is solved. The singular functions added to the analytical solutions are the same singular functions used in the FE analysis.
    - Test the ISBFM code. Problem (52) is solved. The singular functions added to the analytical solutions are different singular functions than singular functions used in the FE analysis.
- The numerical integration for singular functions. It has been studied the convergence of solution when it's necessary to compute an integral with singular function
- The effect of the number of singular functions used in the FE analysis is assessed.
- The blending functions effect is studied too. The blending function distance effect is assessed.

All of this test have been done using lineal elements and elements with $\mathrm{p} > 2$ in order to know the performance of *ISBFM* for high order elements.

4.1. Mesh convergence

FEM convergence

The Matlab code developed is able to solve problems applying the *isoparametric FEM*. Figure 7 shows the mesh convergence in which the error is defined in norm L^2. the problem defined in equation (50) has been solved for different element sizes and different element orders.

The error in norm L^2 is defined in equation (54).

$$\|\mathrm{e}\|_{L^2(\Omega)} = \sqrt{\int_{\Omega} (u - \overline{u})^2 \, d\Omega} \tag{54}$$

Note that in equation (54) u is the analytical solution of the problem manufactured defined in equation (49) and $\overline{u}$ is the solution obtained by *FEM*.

In a square domain of unity length the following element sizes (p) and element orders (h) have been applied:

- $p = 1$ and $h = 2^{-i}$ for $i = 1, 2, \dots 5$
- $p = 2$ and $h = 2^{-i}$ for $i = 1, 2, \dots 5$
- $p = 3$ and $h = 2^{-i}$ for $i = 1, 2, \dots 5$
- $p = 4$ and $h = 2^{-i}$ for $i = 1, 2, \dots 4$
- $p = 5$ and $h = 2^{-i}$ for $i = 1, 2, 3$

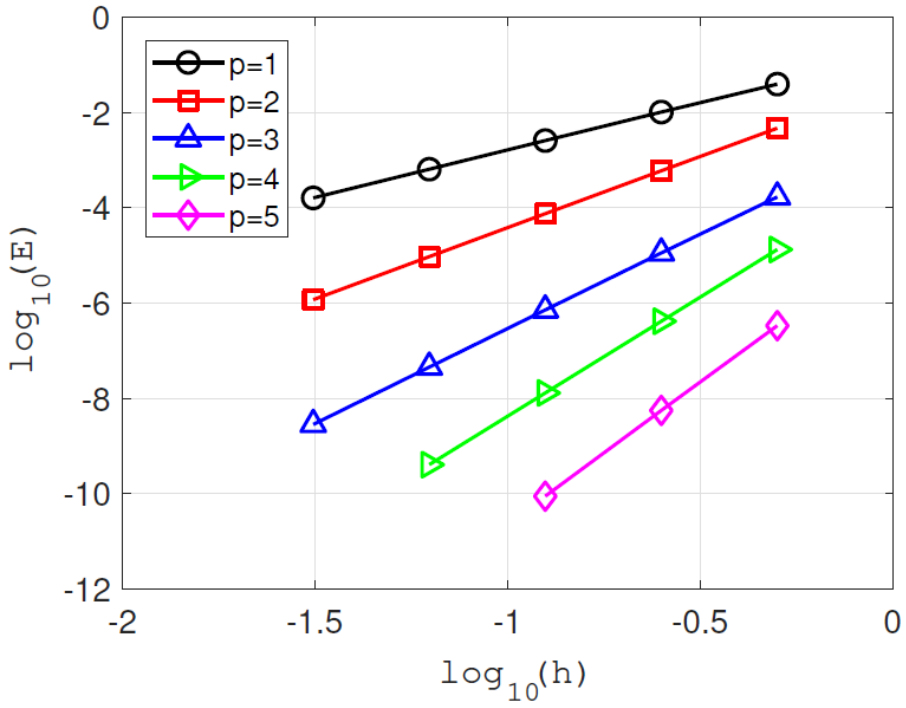

Figure 7. FEM mesh convergence

As it explained in [11] the logarithm of the error L^2 of solution obtained by FEM decrease with slope $p + 1$ when the mesh is refined ($\log_{10}(h)$). In Figure 7 each straight line corresponds to the error in norm L^2 for each element order employed. And the gradient of each straight line decrease as it expected. Thus, the Matlab code has been implemented correctly.

ISBFM convergence

After the *isoparametric FEM* formulation implemented in the code has been verified it has done a similar test to validate the *ISBFM* formulation implemented. To do that, the problem shown in (52) has been solved. In this case, j > 2 for the solution defined in (51) in order to avoid the singular functions in the integrals to compute. This function has been applied around a point located in [0.5 0]. In the solution defined in (51) the equation that defines the singular shape functions (23) is included, then if the function N_s^j in the

analytical solution and function N_s^j add to the *ISBFM* equation system (36) are equal the error in L^2 should be the same error obtained for the previous problem.

So, in Figure 8 is shown the error in norm L^2 for the element size and element order employed previously. Besides 4 functions N_s^j have been added for $j = 1, 2, 3, 4$. Any blending function has been applied.

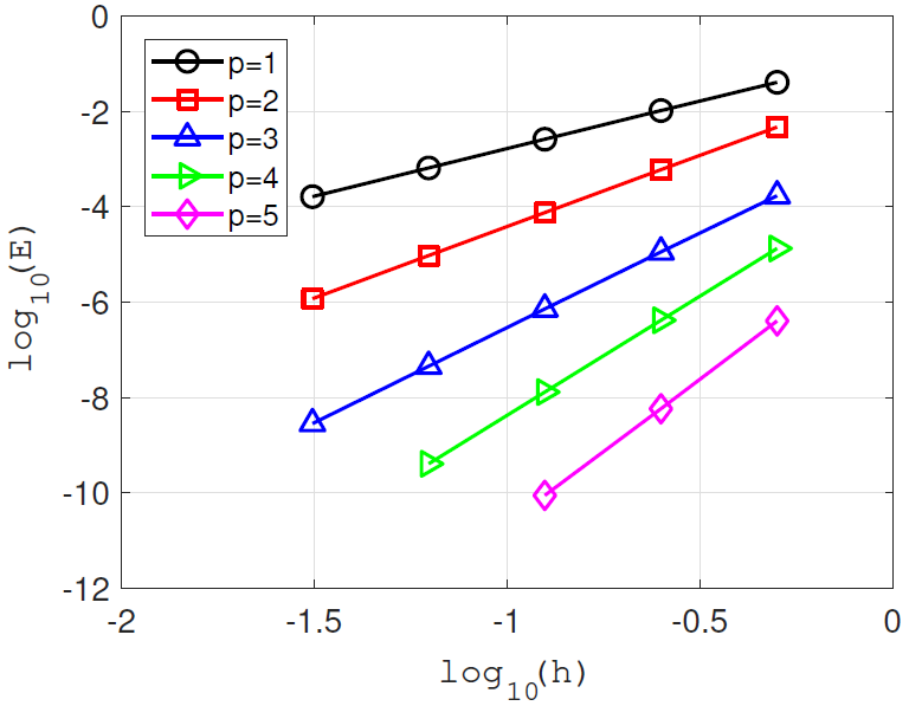

Figure 8. ISBFM mesh convergence. N_s^j used are equal.

Figure 7 and Figure 8 show that the error obtained for both problems is the same value. That means the *ISBFM* formulation has been implemented adequately because the method can reach the *FEM* solution whether the shape functions N_s^j employed are the same functions N_s^j added to the analytical solution.

The *isoparametric FEM* and the *ISBFM* formulations implemented in the Matlab code have been verified. However, in several cases the solution is completely unknown, then the second case has been solve but the functions added in the analytical solution and the functions added in the *ISBFM* equation system are different.

- N_s^j for $j = 1, 2, 3, 4$ added to analytical solution.
- N_s^j for $j = 5, 6, 7, 8$ added to *ISBFM* equation system.

The error in norm L^2 expected for this problem should be higher due to the *ISBFM* can't be reach the exact solution of the functions N_s^j added to the analytical solution. Figure 9 shows the error in norm L^2 for the third problem computed.

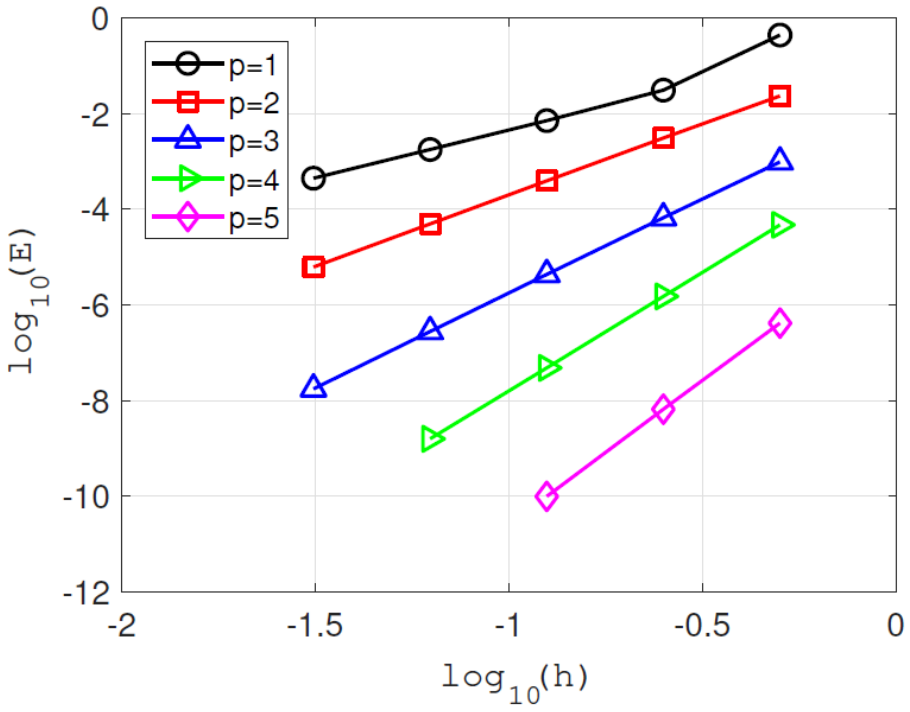

Figure 9. ISBFM mesh convergence. N_s^j used are different.

The error L^2 increase in Figure 9 as it was expected. The difference between Figure 9 and Figure 8 is a consequence of the equation system can't reach the exact solution due to the functions $\mathrm{N_s^j}$ added to the analytical solution are different than the functions $\mathrm{N_s^j}$ employed in the *ISBFM* formulation.

Motz problem convergence

The *ISBFM* formulation has been tested employing the method of manufactured solution without singular functions. Then, to test the Matlab code developed in a case with singularity and without the need to apply special quadratures for singular functions the Motz problem presented in [1] and shown in Figure 3 has been solved. The analytical solution is unknown for this problem, then an element size of 2^{-5} and elements of order 5 have been used to take it as the reference solution in order to compute the error in norm L^2. Figure 10 shows the convergence of error for this problem.

In Figure 10 can be appreciated that the convergence of error is similar to the problems solved before. Each straight line corresponds to each element order employed to compute the problem and the gradient of each line is $\mathrm{p}+1$ approximately as it was expected. Note that the line of $\mathrm{p}=2$ doesn't present the slope farer to $\mathrm{p}+1$ $(2{,}68)$. That can be due to numerical errors because the rest of lines are near to $\mathrm{p}+1$.

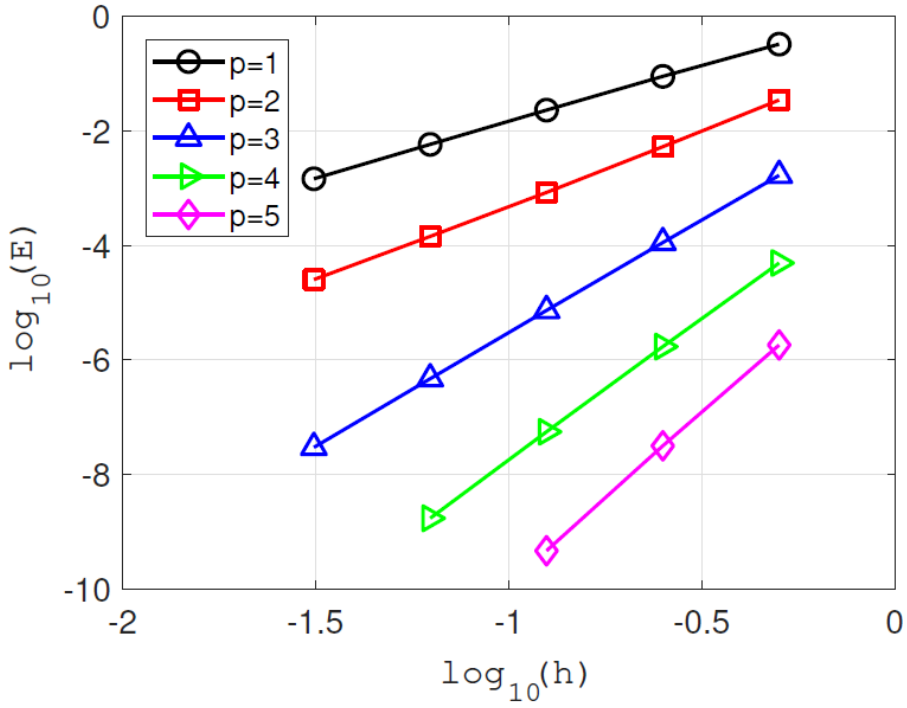

Figure 10. Motz problem mesh convergence.

In spite of the problems solved in *ISBFM convergence* don't contain singular functions, the formulation implemented to compute the solution was equal than formulation use to compute the Motz problem. Then, the results obtained in this section validate the ISBFM formulation developed that has been implemented in the Matlab code to verify it.

4.2. Numerical integration

The Gauss-Legendre quadratures can integrate exactly polynomial functions. However, the shape functions defined in equation (23) are not polynomial. As a consequence of that, it has been assessed the number of points are needed in order to compute this kind of functions with high accuracy.

The shape functions defined in (23) can be singular functions or non-singular functions. That depends on the value of j in equation (23). Whether $j > 1$ there isn't any integral with singular functions. Thus, Gauss-Legendre quadratures are viable to apply.

However, for $j = 1$, integrals on segments adjacent to singular point can't be computed as the others due to the derivate of shape function N_s^j is a singular function. In a consequence a special quadrature or a high number of points of Gauss-Legendre quadrature is needed as it has been exposed in section 3.4.

Due to that, the problem defined in equation (52) has been solved employing different values of j for the analytical solution exposed in (51). Then, the problem defined in (52) have been solved including singular functions and without singular functions.

Non-singular functions

The equation defined in (23) is the product of a square root and a cosine function. Then the Gauss-Legendre quadrature can't integrate exactly them. But, if a reasonable number of points is employed the integration will have a high accuracy. The first case solved in section *ISBFM convergence* has been solved employing different number of points (n) to define the Gauss-Legendre quadrature. Then, for $p = 4$ has been employed the number of point defined in equation (55).

$$n \geq \frac{p+1}{2} + P_e \quad \text{for} \quad P_e = 2,3,4,5 \tag{55}$$

Note that it has been computed the problem until $P_e = 9$ but there isn't appear any improvement from $P_e = 4$.

Figure 11 shows the effect of number of integration points employed to solve the problem.

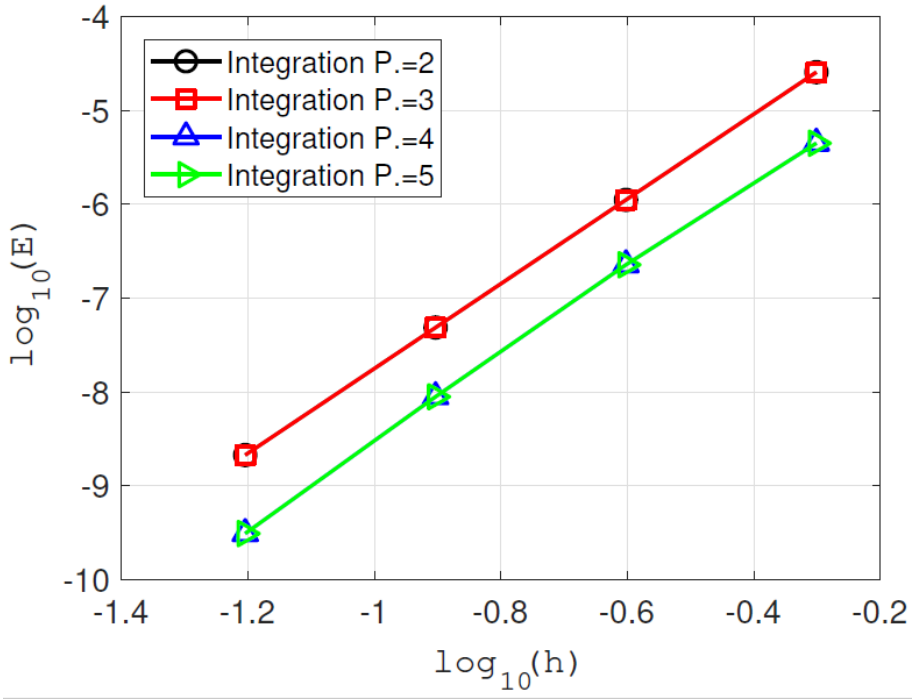

Figure 11. Effect of integration point's number. Non-singular functions

As it is shown in Figure 11, to solve the problem proposed it's recommended use 4 or more points extra (P_e). If it is used less than 4 point extra in order to compute the integral with the function defined in equation (23) the solution obtained will be less accuracy.

Note that the extra points added to compute the integrals depends on the elements order and the value of j employed in equation (23).

Singular functions

In section *Quadratures for singular functions* it has been exposed how to compute integrals with singular functions. Any special quadrature has been implemented in the Matlab code developed, nonetheless the way chosen to compute this integrals is use a high number of points used in Gauss-Legendre quadrature.

In the previous tests done it wasn't necessary compute integrals with singular functions. But, in a general case it can be necessary to do it. Because of that, the following problem, which include integrals with singular functions, have been computed employing a different number of points used in Gauss-Legendre quadrature.

- The strong form of the problem is defined in equation (52).
- The analytical solution is defined in (51) for $\mathrm{j} = 1$. The singular functions used in *ISBFM* formulation is the same.
- The element order employed is 1.
- The problem has been computed using two different number of point (n) for the Gauss-Legendre quadrature: $\mathrm{n} = 8$ and $\mathrm{n} = 95$.

Figure 12 shows the convergence of error for the different number of points used. For a reasonable number (8) when there isn't singular functions isn't enough to compute this functions. Whereas, when a high number of points it's used (95) the convergence is adequate, since the gradient of the straight line is $\mathrm{p} + 1$.

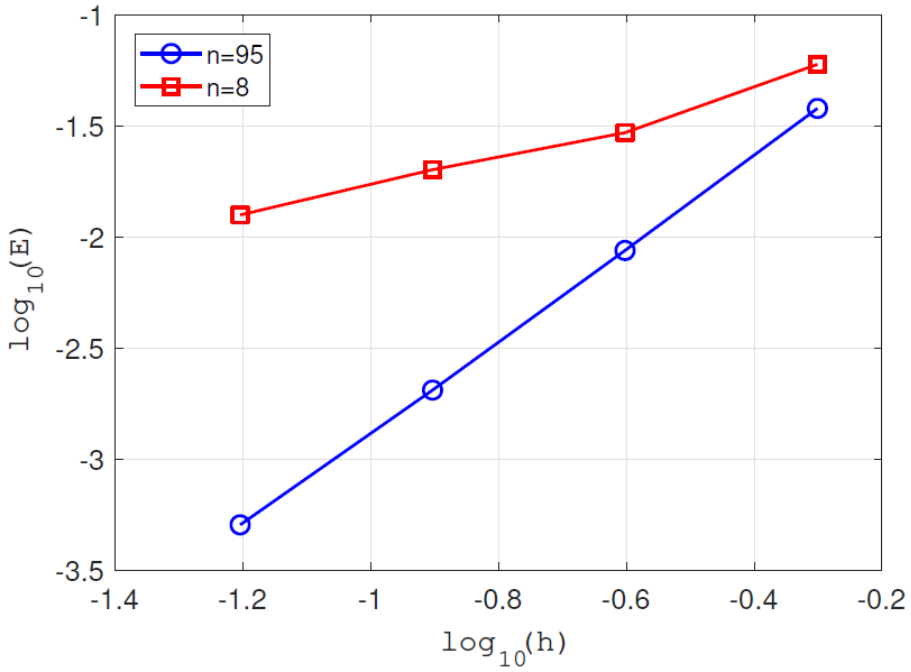

Figure 12. Effect of integration point's number. Singular functions

Figure 13 and Figure 14 show the error L^2 in the domain for the problem computed with a mesh 32x32 elements. Note that for both problems the error is focussed in the singular point located in [0.5 0]. Nevertheless, the error obtained in the problem computed for $n = 95$ is lower.

As a consequence of the results shown in Figure 12, Figure 13 and Figure 14 it is evident that the problems in which it's necessary to solve integrals with singular functions the formulation proposed in section 3 is valid too.

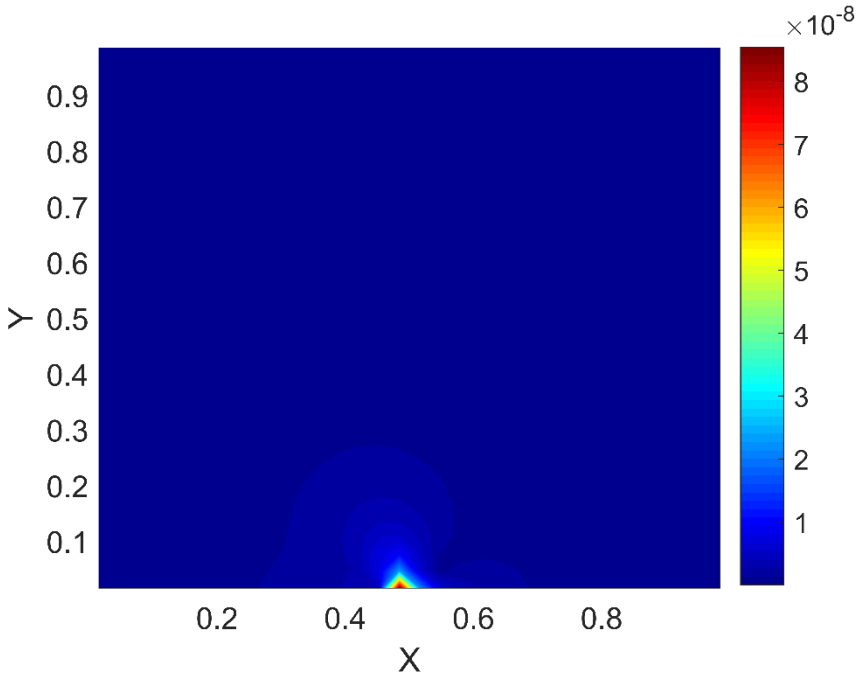

Figure 13. Error L^2 in the domain for n=95.

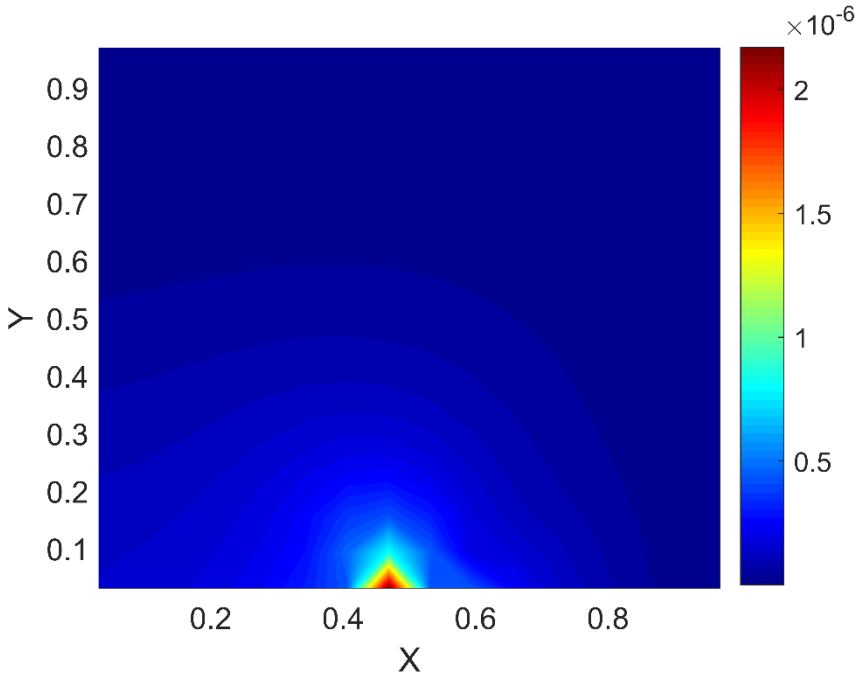

Figure 14. Error L^2 in the domain for n=8.

4.3. Singular functions added

In section *ISBFM convergence* it has been demonstrated that if singular functions employed in the *ISBFM* formulation are equal to the singular functions that are part in the analytical solution, the error obtained applying *ISBFM* formulation would be the error that corresponds to the *isoparametric FEM* calculation. But, usually the singular functions employed in ISBFM are not going to be equal to singular functions of solution. So, two similar test have been done in order to know the effect in the solution obtained when the number of singular functions defined in (23) are employed in the *ISBFM* formulation.

On the one hand, it has been solved the problem exposed in section *ISBFM convergence* using elements of order 1. The solution have 4 singular function defined in (23). Whereas the number of singular functions added to the *ISBFM* formulation goes from 1 to 4. This functions added to the *ISBFM* formulation are the same functions that are in the analytical solution. Figure 15 shows how the error change when singular functions are added to the *ISBFM* formulation.

It can be appreciated in Figure 15 that high number of singular functions employed in the *ISBFM* formulation improve a bit the accuracy of solution. At the moment in singular functions used in both equations are equal the improvement is bigger. Note that the difference between line $\mathrm{ns} = 4$ is the same difference between the straight lines for $\mathrm{p} = 1$ in Figure 8 and in Figure 9.

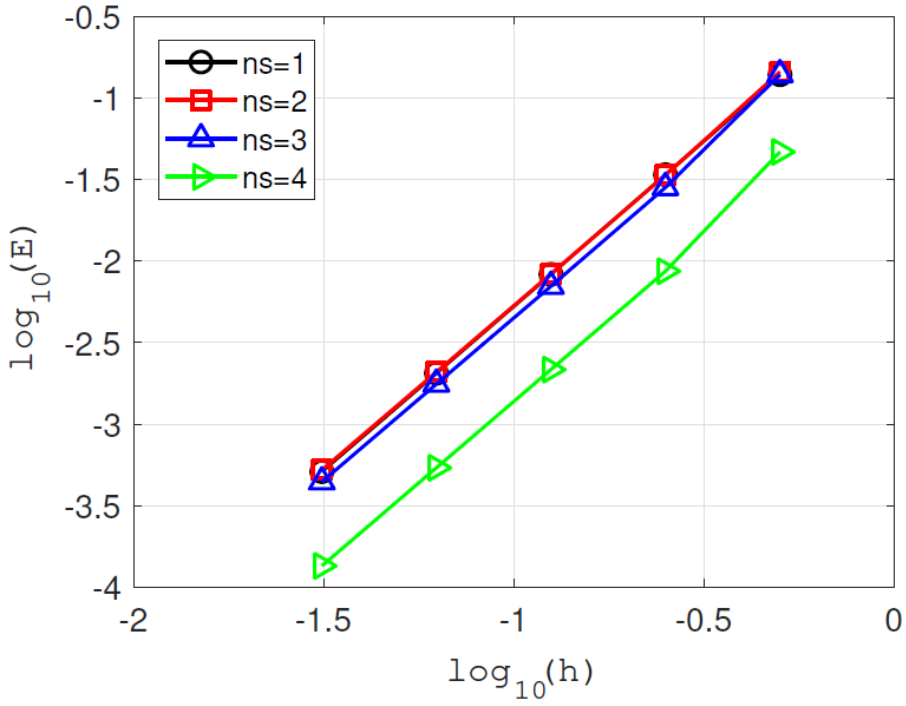

Figure 15. Effect of number of singular functions added. N_s^j used are equal.

On the other hand, the objective of the other test done is the same, but in this case the singular functions employed in the ISBFM formulation are different than singular

functions included in the analytical solution. In this test, the element order has been changed to 4. Figure 16 shows the convergence of error for this problem.

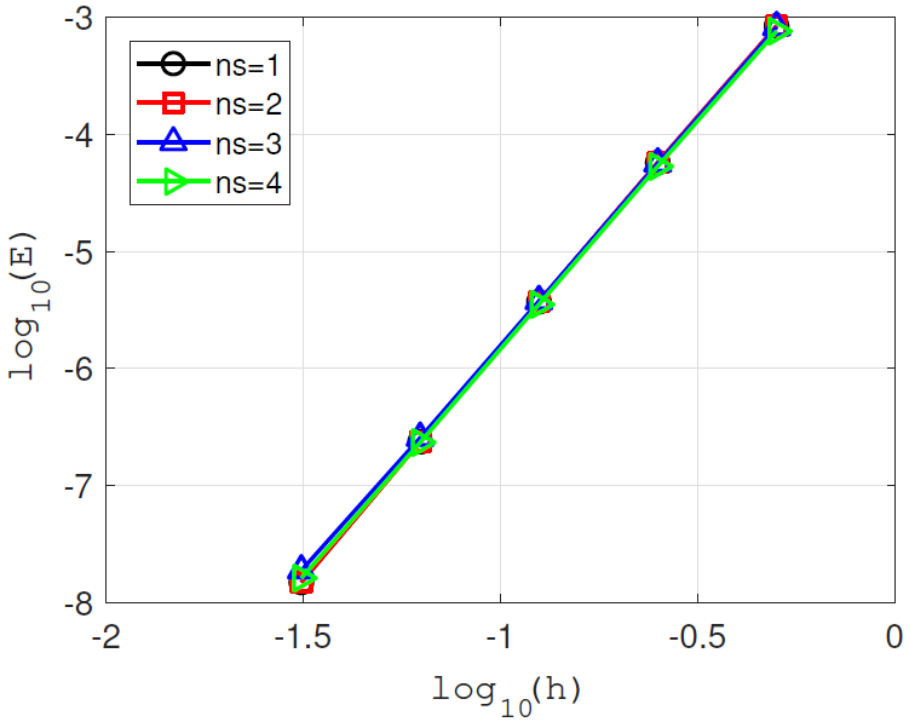

Figure 16. Effect of number of singular functions added. N_s^j used are different.

Note in Figure 16 that the effect of number of singular functions employed in the *ISBFM* formulation have been reduced respect the previous test. In this case, in which singular functions don't match, add a high number of them doesn't lead to a reasonable high accuracy. That is due to the high order elements in *FEM* reach a high accuracy too. Then, a low number of singular function is enough in order to obtain an acceptable accuracy.

4.4. Blending effect

In section 3.5 the blending functions have been introduced. The goal of these functions is reduce the computational cost. That is achieved due to the blending functions limits the area where the singular functions implemented in the *ISBFM* formulation have effect. However, the use of them leads to a loss of accuracy in the solution. The blending function (46) and (47) defined in section 3.5 have been assessed and the results obtained are shown in section Blending function 1 and in section Blending function 2 respectively.

Blending function 1

The first blending function defined in equation (46) has been assessed employing elements of order 1 and 3. The conditions of the problem are:

- 2 singular functions employed. Same functions for the ISBFM formulation and the analytical solution.
- Singular point located in [0.5 0].
- Value of R used for $\mathrm{p} = 1$: $\mathrm{R} = 2^{\mathrm{i}}$ for $\mathrm{i} = 1, 2, \ldots 5$
- Value of R used for $\mathrm{p} = 3$: $\mathrm{R} = 2^{\mathrm{i}}$ for $\mathrm{i} = 2, 4, 6, 8, 10$

Figure 22 and Figure 23 show the effect of blending function for the problem exposed employing two different element order. It can be appreciated that the effect of blending function is considerable. Note that the domain of the problem is small [1 1] and due to that the blending function has produce a high effect.

In both figures can be observed that the convergence of error starts like the no-blending solution but change to become stuck. That is due to the solution goes from to the *ISBFM* solution to the *FEM* solution and the last one has a higher error. Because of that, when the R is increased the value of error where is stuck is lower. Moreover, the increment of element order leads to a high loss of accuracy.

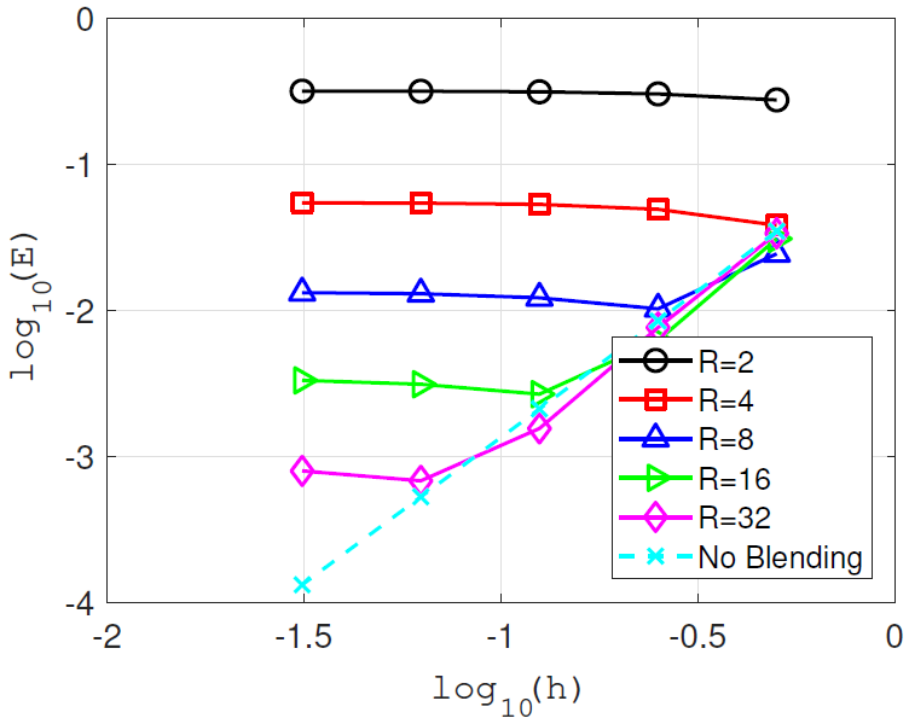

Figure 17. Blending function 1 effect. Element order is 1.

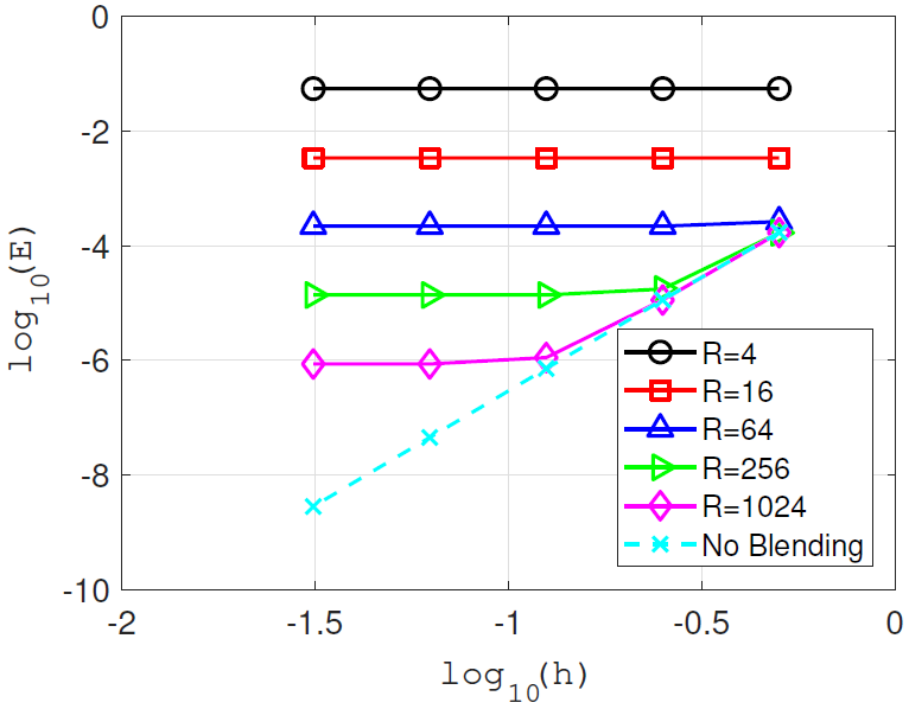

Figure 18. Blending function 1 effect. Element order is 3.

On the other hand, Figure 19 shows how the error is stuck when R is increased. The error for the most refined mesh of each R value has been compared front to R values.

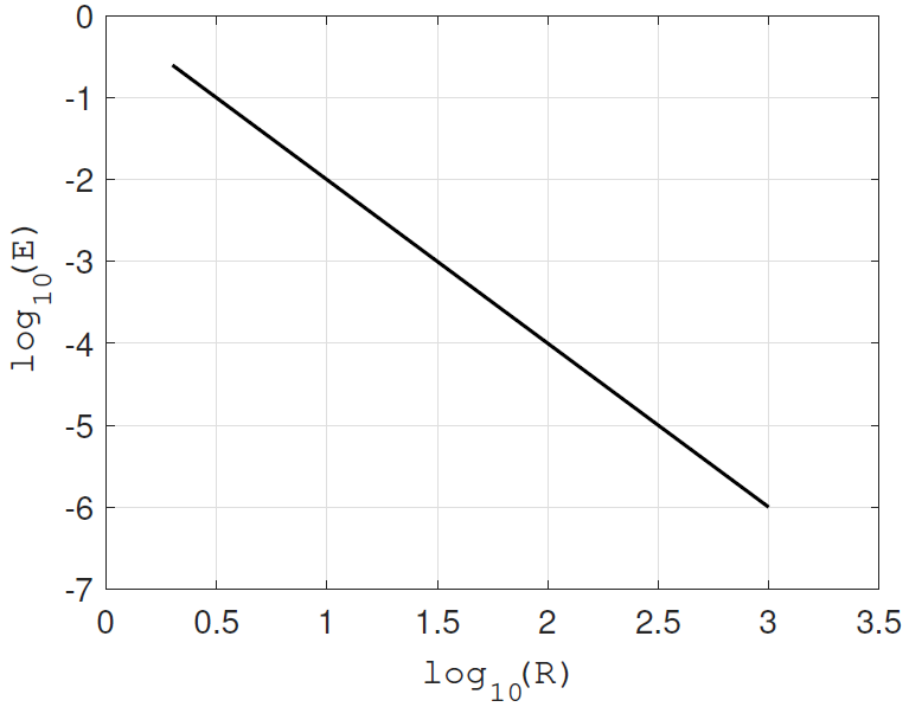

Figure 19. Blending function 1 error front R value.

Figure 19 shows that the error is reduce 2 order of magnitude when the value of R is increased one order of magnitude for an element size: $h \to \infty$. In case the error obtained using a blending function match with the error obtained without use it, increase value of R doesn't have any effect.

Blending function 2

The second blending function defined in equation (47) has been assessed employing elements of order 3. The conditions of the problem are the same than used before. This second blending function have been assessed in order to know the difference between them.

Figure 20 shows the effect of blending function defined in (47). As it has been concluded in [1], the second blending function presents a better performance. The value of error in which the solution is stuck is lower as it is shown in Figure 21 too. As it happened in the previous problem, the error decrease twice when the R increase once.

As it was expected, the application of blending functions leads to a loss of accuracy. Due to that, the use of this kind of functions depends on the problem and the ratio accuracy - computational cost.

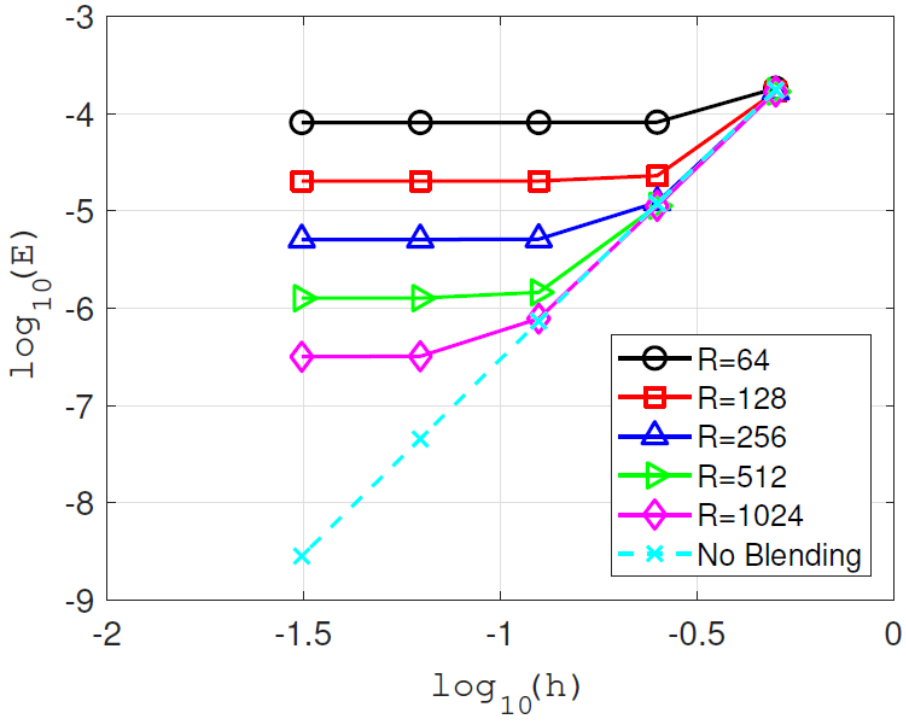

Figure 20. Blending function 2 effect. Element order is 3.

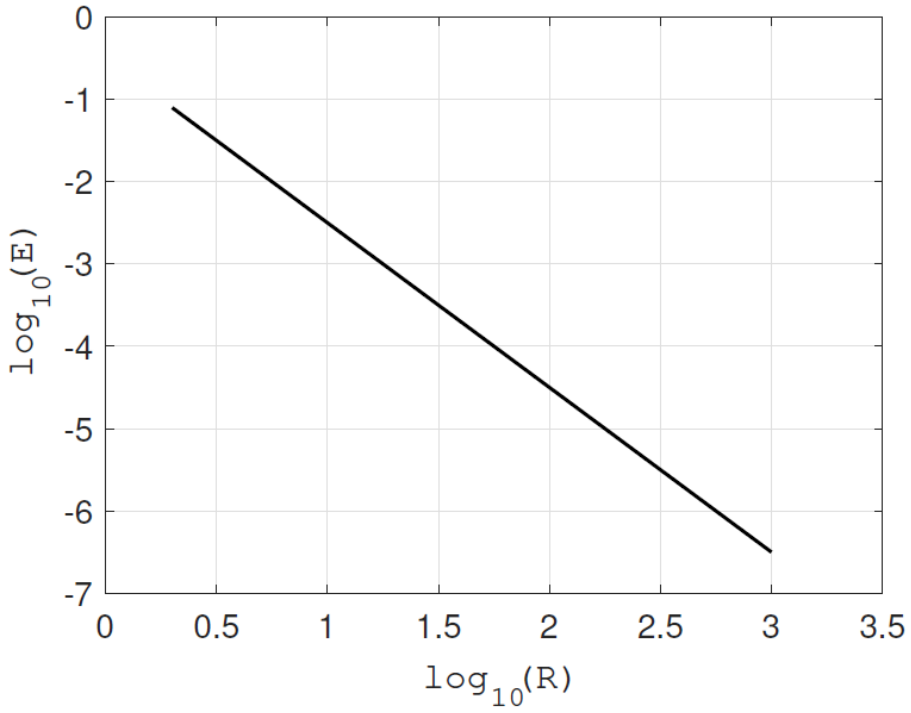

Figure 21. Blending function 2 error front R value.

4.5. Node and singularity placement

The singularity in all tests that have been done was located in [0.5 0]. However, the singularity placement maybe doesn't match with a node, overall if it would be applied in *NEFEM.* Because of that, it has been tested the effect of location of singular point. As it has been previously, this test have been done for two different element order, in this case for $\mathrm{p} = 1$ and $\mathrm{p} = 4$. Besides, the singular functions employed in the ISBFM formulation are different that singular functions that are included in the analytical solution. In this case, the singular functions employed are:

- Singular functions introduced in the *ISBFM* formulation are defined in equation (23) for $\mathrm{j} = 3, 4$.
- Singular functions that are included in the analytical solution are defined in equation (23) for $\mathrm{j} = 2, 3$.

Then, the locations of singular point that have been assessed are the following:

- Singular point located at [0.5 0].
- Singular point located at [1 0].
- Singular point located at [0.1 0].
- Singular point located at [0.25 0].
- Singular point located at [1/3 0].

Figure 22 shows that the location of singularity doesn't have effect in the solution obtained. It is necessary remark two points.

- It has been applied the manufactured method, then the singularity placement is located perfectly and the boundary conditions are well-known.
- Furthermore, the singularity placement doesn't match with a node in all meshes generated for each location of singularity.

On the other hand, Figure 23 shows that the effect of singularity placement in the solution is null. Moreover, in this case the mesh has been kept and the order of element increased, then more nodes match with the location of singularity than in the previous test.

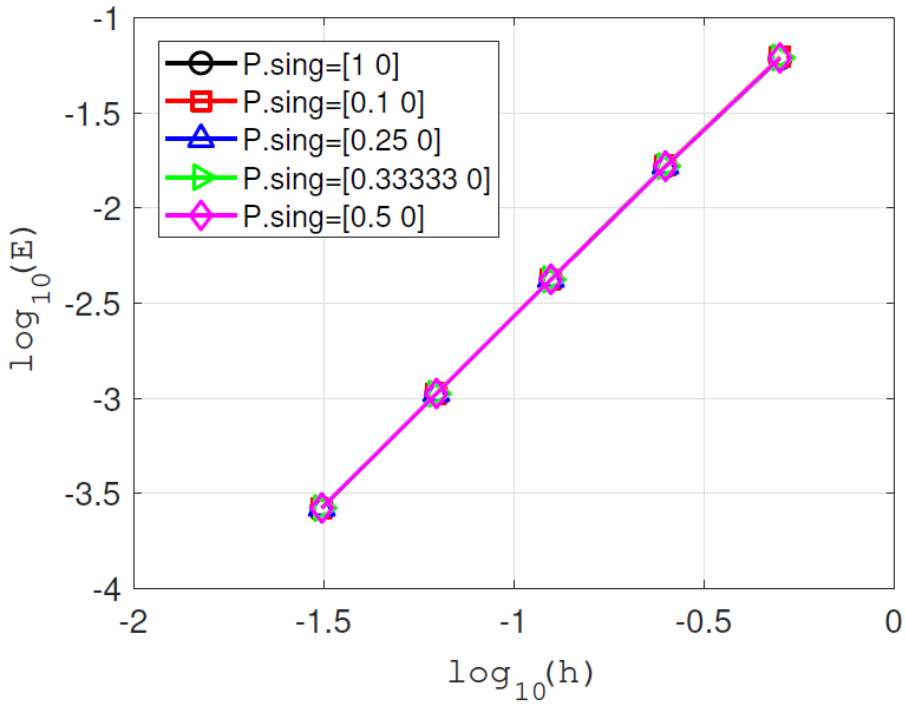

Figure 22. Effect of singularity placement. Elements of order 1.

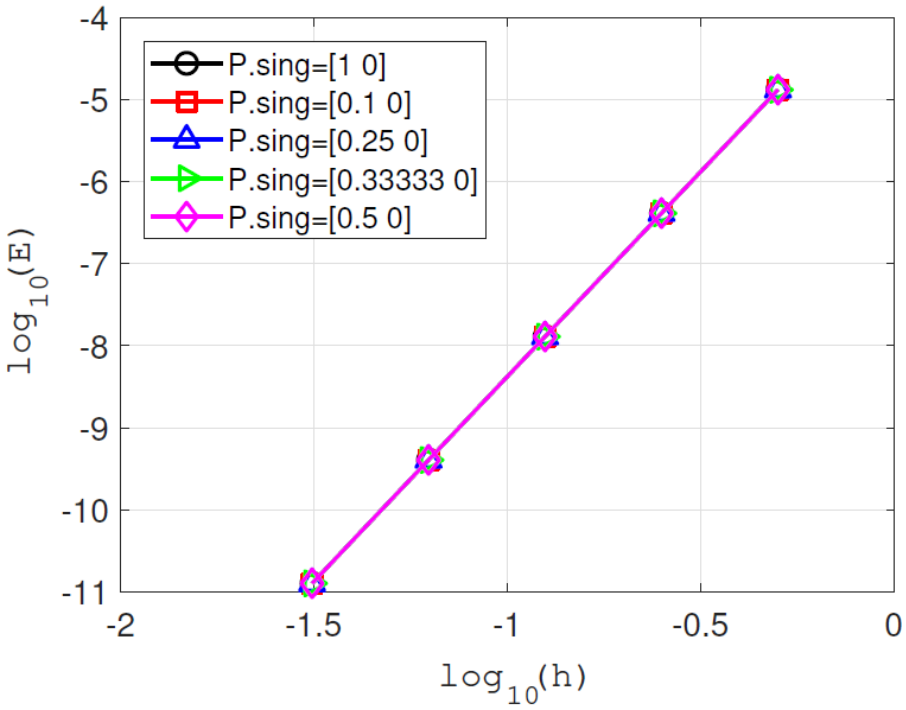

Figure 23. Effect of singularity placement. Elements of order 4.

Remark that the exact location of singularity doesn't affect to formulation developed in section 3.3. The integrals defined in that section in order to compute the *ISBFM* are affected by the boundaries adjacent to the singular point, but not by the exact location of singularity. Because of that, the results obtained in this two test are reasonable.

In Figure 24 and Figure 25 are shown the two possible cases. In Figure 24 the singular point math with a node, whereas in Figure 25 the singular point doesn't match with a node.

In Figure 24 the element order is 1, employing a mesh 6x6 in the domain [1 1] and the singular point is located in [1/3 0].

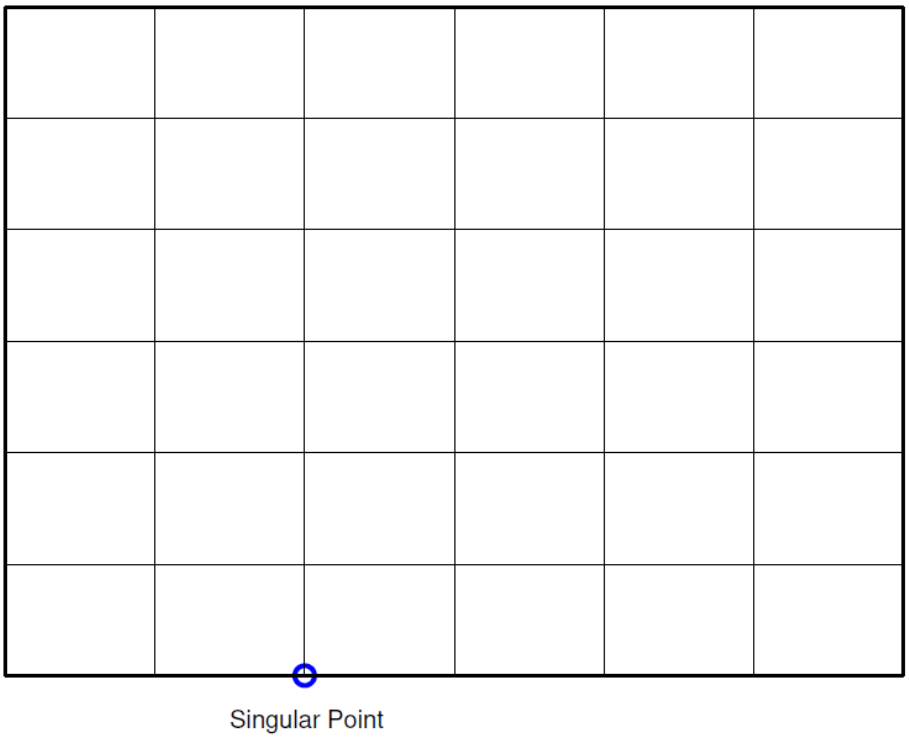

Figure 24. Singular point matchs with a node

In Figure 25 the element order is 1, employing a mesh 8x8 in the domain [1 1] and the singular point is located in [1/3 0].

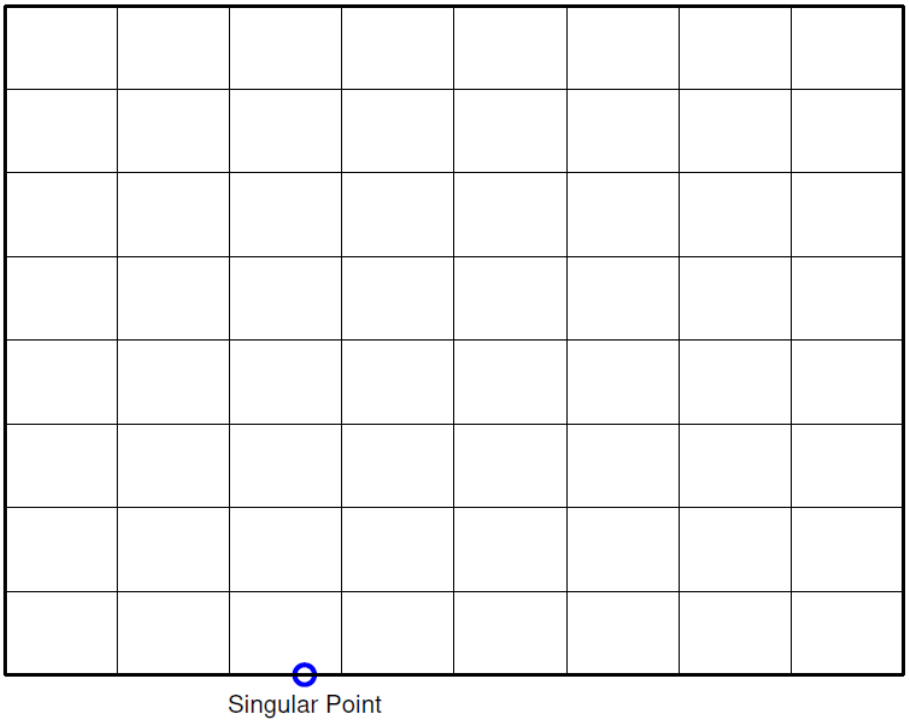

Figure 25. Singular point doesn't match with a node

5. CONCLUSIONS

The *ISBFM* formulation proposed in [1] have been expanded in order to solve any kind of problem in which appears a singularity. The formulation proposed in section 3 have been validate by the test exposed in section 4. The most relevant conclusions obtained are summarized next:

- **ISBFM applied for general cases**. The tests done in section 4 show that the convergence error presents a slope $p + 1$ as it was expected [11]. The *ISBFM* formulation preserving the formulation of *isoparametric FEM*. Due to that, the error obtained is a sum of errors of both methods. And then it can be deduce that the weak formulation presented in section 3.2 can be applied with *isoparametric FEM* or with other FE method.

- **Integration of singular functions.** As it was predicted in section 3.4 the apparition of integrals with singular functions will need a different numerical integration than it has been defined in section *Numerical integration*. The test done in section 4.2 bear out that it is necessary to use special quadratures to compute this kind of integrals in order to achieve an adequate convergence of error.

- **Number of singular functions employed**. Employ a low number of singular functions (23) in the *ISBFM* formulation it's enough to reach an acceptable accuracy. In section 4.3 it's shown that there isn't a reasonable accuracy improvement when the number of singular functions employed is increased.

  If the singular functions used in the *ISBFM* formulation were the same singular functions which defines the singularity, the error due to *ISBFM* would be null. Nevertheless, this scenario is not frequent.

- **Blending functions effect**. In section 3.5 the blending functions have been introduced. The goal of this functions is reduce the computational cost. However, as it has been deduced in [1], the use of this functions lead to a loss of accuracy. Moreover, when the elements order is increased, this loss is greater.

- **Singularity location**. In the example presented in [1] the singularity location match with a node. Nonetheless, in some problems the placement of singularity can no match with a node, for example whether *NEFEM* is applied. Because of that, the section 4.5 has been focussed in test the effect of singularity location and the results obtained have evidenced that it isn't necessary that singularity location match with a node.

- **High-order elements effect**. The perks of use high-order elements in *isoparametric FEM* are preserved in the *ISBFM* formulation proposed.

Besides, the use of high order elements leads to reduce more the small effect of number of singular functions used. On the other hand, the use of blending functions and high-order elements together entails a higher loss of accuracy as it has shown in section 4.4.

To conclude, the *ISBFM* weak formulation proposed in section 3.2 allows to solve problems which presents singularities, reaching an acceptable accuracy, without the necessity to refine the mesh, it isn't necessary that singular location match with a node and the use of high-order elements is worth. However, in some many cases it will have to apply specific quadratures for singular functions. Due to that, the method proposed can be a good option to use with NEFEM at the same time.

6. FUTURE DEVELOPMENTS

Along this thesis *ISBFM* has been assessed in order to know its performance in problems in which *NEFEM* would be applied. That is not enough to determinate that *ISBFM* is the option to apply in *NEFEM* to solve problems in which the solution is non-smooth due to singularities. Thus, some researches lines are still open:

- **Numerical integration**. As it has been commented in section 3.4 some kind of problems can't be solved properly using Gauss-Lagendre quadratures. In case the boundaries conditions alongside the singularity's boundary can't be homogeneous it is necessary to apply specific quadratures to integrate singular functions. Then, the integration of this kind of integrals in *NEFEM* deserves more attention in order to evaluate whether *ISBFM* could be applied in this situation.

- **Test ISBFM and NEFEM together**. The *ISBFM*'s performance have been tested in the *isoparametric FEM* code developed on purpose. Thus, test it in the NEFEM will validate the results obtained in this thesis.

- **Assess other methods**. In this thesis only one method to solve problems with singularities have been studied. Nevertheless, other methods, like *GFEM/XFEM* [3], have been developed in the last decades to solve this kind of problems. So, it is worth to assess other methods in order to compare among them. Thus, it will help to choose the method that fits better with *NEFEM*.

7. REFERENCES

1. Lorraine G. Olson, Georgios C. Georgiou, and William W. Schultz, *An Efficient Finite Element Method for Treating Singularities in Laplace's Equation* (Journal of Computational Physics 96, 391-410 (1991)).
2. Miltiades Elliotis, Christos Xenophontos and Georgios C. Georgiou, *Numerical Solutions of Laplacian Problems over L-Shaped Domains and Calculations of the Generalized Stress Intensity Factors* (Fifth World Congress on Computational Mechanics July 7-12, 2002, Vienna, Austria).
3. Thomas-Peter Fries and Ted Belytschko, *The extended/generalized finite element method: An overview of the method and its applications* (Int. J. Numer. Meth. Engng 2000; 00:1–6).
4. Ivo Babuška, Uday Banerjee and John E. Osborn. *Generalized Finite Element Methods: Main Ideas, Results, and Perspective.*
5. Shogo Nakasumi, Katsuyuki Suzuki and Hideomi Ohtsubo. *Crack growth analysis using mesh superposition technique and X-FEM*. (International Journal for Numerical Methods in Engineering 75, pp. 291-304, 2008).
6. Jens M. Melenk. *Hp-Finite Element Methods for Singular Perturbations.* (Springer Science & Business Media, 10 Oct. 2002)
7. T. Eibner, J. M. Melenk. *An adaptive strategy for hp-FEM based on testing for analyticity.* (Comput Mech (2007) 39:575–595).
8. Patrik Daniel, Alexandre Ernz, Iain Smears, Martin Vohralík. *An adaptive hp-refinement strategy with computable guaranteed bound on the error reduction factor*. (arXiv:1712.09821v2 [math.NA] 21 Apr 2018).
9. Rubén Sevilla, *Doctoral Thesis NURBS-Enhanced Finite Element Method (NEFEM)* (Universitat Politècnica de Catalunya. Programa de Doctorat de Matemàtica Aplicada. Departament de Matemàtica Aplicada III (July 2009)).
10. Babuška, I. and Szabó, B. A., *On the Rates of Convergence of the Finite Element Method.* (International Journal for Numerical Methods in Engineering 18, pp. 323-341, 1982).
11. Xue D, Demkowicz L. *Control of geometry induced error in hp finite element (FE) simulations. I. Evaluation of FE error for curvilinear geometries*. (International Journal for Numerical Analysis and Modelling 2005; 2(3):283–300).
12. Ruben Sevilla, Sonia Fernández-Méndez and Antonio Huerta. *Comparison of high-order curved finite elements.* (Int. J. Numer. Meth. Engng 2011; 87:719–734).
13. TP Chandrupatla & AD Belegundu*, Introduction to finite elements in engineering,* (Prentice-Hall, Englewood Cliffs, N.J., 1991).
14. Aurelia Cuba Ramos, Alejandro M. Aragón2, Soheil Soghrati, Philippe H. Geubelle and Jean-François Molinari. *A new formulation for imposing Dirichlet boundary conditions on non-matching meshes* (Int. J. Numer. Meth. Engng (2015)).
15. Dr. Rubén Sevilla. Finite Element Computational Analysis EG-M23. Swansea University, College of Engineering.

16. https://pomax.github.io/bezierinfo/legendre-gauss.html (Acceded: 14/11/2018).
17. Tema 3. Interpolación. Funciones de forma de continuidad C^0. Técnicas computacionales. Universidad Politécnica de Valencia, ETSID.
18. Daan Huybrechs and Ronald Cools. *On generalized Gaussian quadrature rules for singular and nearly singular integrals.* (Report TW523, May 2008).
19. Sumlearng Chunrungsikul, *Doctoral Thesis Numerical Quadrature Methods for Singular and Nearly Singular Integrals.* Department of Mathematical Sciences, Faculty of Technology and Information Systems, Brunel University (October 2001).